Mohamed Khider University of Biskra
Faculty of Exact Sciences and Natural and Life Sciences
Material Sciences Department

MASTER MEMORY

Domain: Material Sciences
Branch: Physics
Specialty: Material Physics

Ref.: Enter the document reference

Presented by:

Walid REGUIAI

The: June 2024

Study on the Structural, Optical and Electrical Properties of pure NiO and La-doped NiO, prepared by sol-gel method.

Jury :

Mr.	**LAKEL Abdelghani**	MCA	University of Biskra	President
Mr.	**LAKEL Said**	Pr	University of Biskra	Supervisor
Mrs.	**ALMI Kenza**	MCA	University of Biskra	Examiner

Academic year : 2023-2024

Acknowledgments

This master's thesis work was carried out at the Laboratory of Semiconductor and Metallic Materials (LMSM) of Mohamed Khider University of Biskra. Through this modest memoir. First of all, I thank my God Allah who made it easier for me to complete this work.

I would dedicate deep thanks and grateful to my supervisor **Pr. LAKEL** Said who has been like a beacon through continuous follow-ups, he has been really kind and helpful effort and encouragement.

I desire to express my gratitude to **Dr. LAKEL Abdelghani** and **Dr. ALMI Kenza** of Mohamed Khider University of Biskra, for having agreed to examine my research work and to be part of my dissertation jury.

I am eager to thanks all members of the Laboratory of Semiconductor and Metallic Materials (LMSM), and may they receive the expression of my deep gratitude for the pleasant atmosphere.

I would also like to thank very much all the teachers in the Physics department specializing in Materials Physics at Mohamed Khider University of Biskra who taught me during my academic career, where I gained a wealth of experience, practical and scientific ideas.

I don't forget to thank my dear colleague’s physician graduating class 2022-2024 of Mohamed Khider University of Biskra, everyone who helped me directly or indirectly over the course of my studies.

Finally, I would like to express my sincere thanks to my family, friends and to all those who have helped me accomplish this research work.

Table of contents

Pages

Chapter II. Materials and methods

Chapiter III. Results and Discussion

General Introduction

The developments of the thin films and their applications made the technological revolution in electronics, IT and communications and penetrated in other fields like: medicine and biology, energy production, cars industry, drug delivery...etc. Practically, all the components of any device are manufactured using thin film processes, the impact of this development on modern life is immense.

The investigation of the physical properties of thin films has developed considerably over the last few decades, this branch arose from the diversity of the materials and is distinguished by the particular area studied, the method of investigation and so on. In fact, these continuous investigations and linked advances research was the driving force for the scientific breakthroughs and the significant progress in thin film technologies.

Among a wide range of material classes used to fabricate nanostructures and thin films, transparent conducting oxides (TCOs) based on metal oxides of simple, binary and multiple elements, are showing as one of the most advantageous families with many suitable properties. The key properties of TCOs include good electrical conductivity and high transparency in the visible spectrum of light, has grown in importance in several device technology especially in optoelectronic and photonic devices applications.

Presently, metal oxides have attracted a lot of attention due to their distinctive physical, chemical, optoelectronic features [1]. A p-type metal oxides transparent semiconductors play a pivotal role in optoelectronics and block electronics applications, but the deficiency of a high-performance one still remains as an obstacle to the development of future generation optoelectronics [2]; Nickel oxide (NiO) is an important p-type semiconductor binary with a direct broad bandgap (3.6-4.0 eV), good thermal and chemical stability as well as large optical transparency [3]. Its powerful uses in gas sensors, photocatalysis, electrochromic coatings, solar cell, UV photo-detector, heterojunction LEDs [4-6]. Nevertheless, its applicability is often limited due to low electrical conductivity and carrier mobility.

Therefore, doping NiO with other elements leads to improved their characteristics where some reports and studies on doped oxide semiconductors with trivalent rare-earth ions such as La^{+3}, Er^{+3}, Ce^{+3}, Yb^{+3} are doped on to oxide semiconductors contribute to enhancing their optical properties [7].

In this context, Lanthanum (La) was applied as doping element, it is a rare earth metal element, with different electrical structure where has an electronic configuration including

partially 4f and 5f electron shell, with a relatively high ionic radius such as nickel and thus resulting in lattice strain [8-9]. Earlier studies suggests that lanthanum doping significantly enhances NiO's optical absorbance and electrical conductivity, making it perfect for a broad range in optoelectronic applications [10]. Likewise, La-doped NiO nanofibers synthesized as electrode materials have potential application for high-performance supercapacitors [11].

The physical characteristics of doped thin films are considerably influenced by their shape and crystalline structure, which are basically controlled by the synthesis processes. In this work, we report the synthesis and characterization of pure and La doped NiO thin films grown by sol-gel assisted spin coating technique. The purpose of this work is to synthesis NiO films while reporting and discussing the effect of doping concentration (La %) in terms of structural, optical and electrical properties.

After a bibliographic review of the literature in the first part, the second part of the manuscript describes the sol-gel assisted spin coating technique deposition of pure and La doped NiO thin films, as well as structural, optical and electrical characterization methods. The third part devoted to discussion and interpretation of characterization results of pure NiO thin films, and the influence of lanthanum doping concentration (La %) on NiO films. The last part of the manuscript presents general conclusion that brings together all the main results of this work.

Chapter I: State of the art

I.1 Transparent Conductive Oxides (TCOs):

Over the last few years, scientists have achieved rapid and significant innovations in the branch of material science, notably in metal oxide semiconductor physics. The majority of transparent conducting materials used today are based on different metal oxides referred to as transparent conducting oxides (TCOs), this family are widely considered the most diverse, rich and multifunctional materials, with properties almost covering all characteristics of materials science.

Transparent conductive oxides (TCOs) are a class of materials, refer to any oxide which have the unusual capability of being both transparent in the visible range exceeds 90% and electrically conductive $\geq 10^4\ S.cm^{-1}$ [12], with wide band gap $\geq 3\ eV$ and extremely high doping levels above $10^{20}\ cm^{-3}$ where these doping levels the materials are degenerate semiconductors and show a metal-like behavior [13-14].

The most TCOs are binary or ternary compounds, having one or two metallic elements in combination with oxygen, as they can be produced as n-type and p-type conductive. Suitable oxides must meet three fundamental requirements to be considered as transparent materials with high conductivity:

- They should exhibit a large enough bandgap so that absorption due to band-to band transitions is limited to the UV and will not diminish cell current.
- Suitable extrinsic or intrinsic dopants that form shallow states have to be introducible in a sufficient quantity [15].
- The material should not be liable to formation of compensating defects upon shifts of the Fermi level (Fermi level pinning) [16].

The choice of TCOs based on a number of parameters such as chemical, mechanical and thermal stability, stress, toxicity, low costs. In addition, the scientists succeeded established factors of merit (*FOM*) allows to compare between TCOs; the best known is that defined by the ratio between the electrical conductivity (σ) and the coefficient absorption (α):

$$FOM = \frac{\sigma}{\alpha} = -[Rsq\ .ln\ (T + R)]^{-1} \quad \text{(I.1)}$$

In which Rsq, R and T respectively represent the square resistance, reflectance and transmittance in the visible range of the material used. The high-quality factor *FOM* lies between [0-7], so the best TCO will have high conductivity and low absorption in the visible range [17].

The highest *FOM* is 7 and corresponds to that of fluorine F-doped ZnO, which displays a square resistance of Rsq= 5 (Ω/□) and an absorption coefficient of 0.03 cm^{-1} [12]. According to the literature, the parameters T ≥ 90% and Rsq ≤ 100 (Ω/□) are the minimum standard properties for a material to be marketed as a TCO. These properties are essential for several applications more precisely in optoelectronics, since the TCOs must receive the maximum visible spectrum with high electrical conductivity. There are strategies to improve the performance of existing TCOs, that consists of:

- Improve carrier mobility by choosing the right dopants and doping process.
- Choose the right growth method and conditions.
- Perform post-deposition treatments.

By these strategies, it was possible to control the carrier concentration and transparency properties, as well as broadening the absorption spectrum of the TCOs.

For any application, the most suitable TCO is the one that shows good electrical conductivity along with good optical transparency. The thermal, physical and chemical durability, thickness, plasma wavelength, deposition temperature, toxicity, and cost are other factors that may also influence the select of transparent conducting material for any particular application, as shown from Table I.1 [19].

Table I.1. Minimum required properties of TCOs [20].

Parameters	Transparent conductive Materials
Band gap	**>3.1 eV (380nm)**
Transparency at 550nm	**>90% (for n-type) and > 85% (for p-type)**
Resistivity	**10^{-4}Ω cm (for n-type) and 10^{-3}Ω cm (for p-type)**
Carrier Concentration	**>10^{20} cm^{-3} (for n-type) and >1018 cm^{-3} (for p-type)**
Mobility	**>40 cm2 $(V\ s)^{-1}$ (for n-type) and >20 (V s)-1 (for p-type)**
Sheet resistance	**≤10 kΩ/ square (for 20nm thickness)**

I.1.1 Optical and Electrical Properties of TCOs:

The primary interest to control the charge carrier's concentration and mobility in the TCO film is to present the possibility of an optimization of its electrical properties. This possibility is closely linked to the intrinsic material of the TCO and the type and concentration of dopant. Already, the conductivity (σ) of thin film is highly dependent on the carrier concentration and mobility which are connected by the following relation:

$$\sigma_{n,p} = nq\mu = \frac{ne^2\tau}{m^*} = \frac{1}{\rho} \quad \text{(I.2)}$$

Where n is the density of electron (hole) in conduction band (valence band) expressed in (cm^{-3}), q is the charge of the electron $1.6x10^{-19}$ (C), and μ is the mobility of charge carriers ($cm^2.V^{-1}.s^{-1}$). The second verse show the dependence of material conductivity with the number of charge carriers n, their effective mass m^*, and the relaxation time τ. Moreover, the resistivity (ρ) defined as the inverse of conductivity ($\Omega.cm$), where an important surface electrical property in thin films measurements named surface resistance R_S, defined as the ratio of resistivity (ρ) to layer thickness (d) [12]:

$$R_s = \frac{\rho}{d} \quad \text{(I.3)}$$

The above equation (I.2) proves to become conductive, the films must either outcome essentially from non-stoichiometric or by intrinsic doping such as oxygen vacancies, or more generally, be doped with appropriate external impurities to form an extrinsic doping [22]. The possibility of increasing the conductivity of the films consists either in improving the concentration of carriers by doping, or in improving the electronic mobility μ.

The optical properties of TCO thin films provide powerful tools to known energy band structure, localized defects, impurity levels, lattice vibrations etc. These properties and the optical constants are strongly connected to the deposition parameters, microstructure, level of impurities and growth technique [23-25].

An important characteristic of TCO thin films is the existence of a transmission window covering a wide range of the visible spectrum. The optical window is centered between two characteristic wavelengths where light is no longer transmitted $\lambda gap < \lambda < \lambda p$ (called plasma wavelength) where TCO is transparent has a dielectric type behavior, at short wavelengths near UV range ($\lambda < \lambda gap$), absorption dominated by band-to-band transitions, where at high wavelengths in the near infrared range rang ($\lambda > \lambda p$), the incident light is reflected by the TCO material and behaves like a metal and absorbs or reflects light.

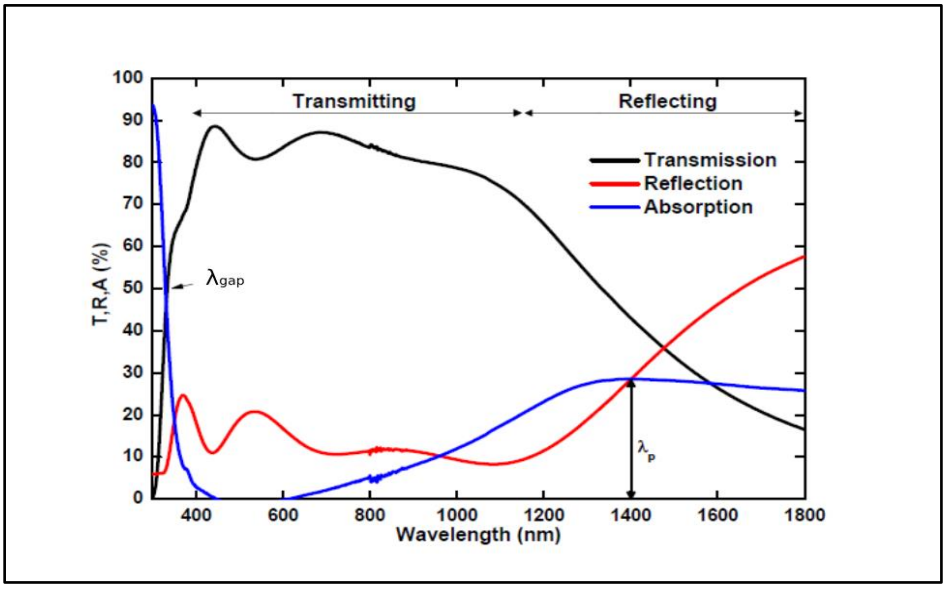

Figure I.1. Transmission, Reflection and absorption spectra of a typical TCO, the optical window and λ_{gap}, λ_p are the wavelengths at which the band gap absorption and free electron plasma absorption takes place [26].

Generally, with TCOs whose plasma wavelength $\lambda_P = \frac{2\pi.c}{\omega_P}$ ..... (I.4) typically between 1 and 2 (µm), the type of oxide and its doping are optimized to have a transparency range ranging from near UV to near infrared depending on the material used and its doping [27]. The doping of TCO will heavily influence the interaction of photons and excitons which shifts in the plasma wavelength and therefore a reduction in the transparency of the TCO in the infrared.

I.1.2 TCOs material and their relevance to some applications:

TCO films have gone through very significant development and are used virtually every day in various applications. The actual and potential applications of TCO thin films include: transparent electrodes for photovoltaic cells, transparent electrodes for flat panel display, transparent thin films transistors, gas sensor, photocatalysis, low emissivity windows, light emitting diodes LEDs and semiconductor lasers.

As an advantage of TCO thin films depends on both their optical and electrical properties, both properties should be considered together with environmental stability, abrasion resistance, electron work function, and compatibility with substrate and other components of a given device, if necessary for the application. The availability of the raw materials and the cost of the deposition method are also important factors to select the best TCO material.

I.2 Nickel oxide (NiO):

Nickel oxide is a chemical compound where nickel occupy 78.55% while oxygen is 21.40%, in the form of black or greenish-gray crystalline powder depending on the method of preparation. As a binary metal oxide, the ratio of Ni:O deviates from 1:1 making it non-stoichiometric most times whilst their stoichiometry is shown by the color variation [28-29]. There are various oxidation states likewise: nickel or nickelous oxide (NiO), nickel dioxide (NiO_2), nickel trioxide or sesquioxide (Ni_2O_3), nickel peroxide (NiO_4) and nickelosic oxide (Ni_3O_4).

NiO is a transition metal oxide has rhombohedral or cubic structure referred to as Bunsenite. Naturally, NiO is a p-type of semiconductor because of nickel deficiency, with a wide band gap between 3.5 to 4.0 *eV* [30]. NiO has a high Neel temperature (523 K) [31], which makes it suitable for room temperature. Due to the simplicity in its synthesis, high durability and excellent chemical stability in any solvent, it has diverse applications.

I.2.1 Fundamental properties of NiO:

I.2.1.1 Structural Properties:

Nickel oxide embraces the rock salt type lattice of NaCl with an octahedral Ni (II) and O^{-2} sites, each cubic unit cell has four nickel atoms and four oxygen atoms. Each nickel atom is bounded by six oxygen atoms and the same thing for oxygen atoms. This face-centered cubic (FCC) structure has a parameter of a= 4.1769 Å at 26 °C. The FCC structure has a primitive rhombohedral cell with α = 60° along anyone of its triad axes where nickel-nickel distance is 2.9518 Å for the distorted rhombohedral (α =60°4.2' at 18°C). The face (111) is polar and therefore non-stable, whereas the face (100) is a stable non-polar face. Ni^{2+} and O^{2-} ions alternate along the direction [111], and magnetisation is linked to the plane (111). Nickel oxide has low magneto crystalline anisotropy. The ionic radii: R (Ni^{2+}) =72.0 Pm and R (O^{2-}) =140 Pm [32-33].

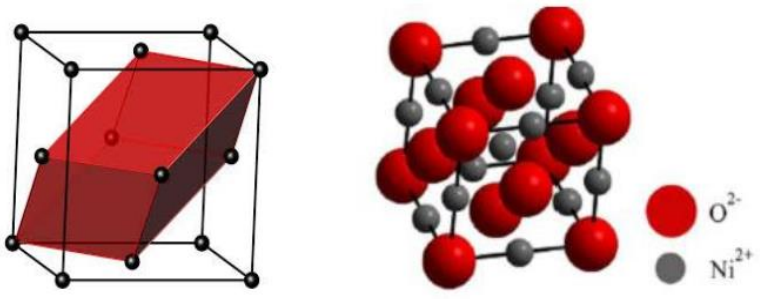

Figure I.2. The FCC and rhombohedral primitive cell of NiO [33].

I.2.1.2 Optical Properties:

Nickel oxide (NiO) is a semitransparent semiconducting material with direct large bandgap in the range of 3.6-4 eV, with refractive index is 2.33 at the photon energy of 2 eV. The absorption edge is localized in the ultraviolet region, the presence of Ni^{3+} ions inner the oxide lattice shows charge transfer transition with the resulting absorption in the visible region [34-36].

The valence band of NiO composed of localized nickel *3d*-bands with a width of 4.3-4.4 eV were coupled with oxygen at the *2p*-bands states with large energy about 4-8 eV. Nevertheless, the conduction band composes of unoccupied states of nickel *3d*, *4s*, and *4p* [37-39]. Two principal theories proposed for interpreting the optical absorption gap in NiO: it is due to either a p→d transition in one Ni atom or a d→ d transition throughout two adjacent Ni atoms in the lattice [40-41].

I.2.1.3 Electrical Properties:

NiO has p-type oxide semiconductor character of the group AVI BVIII, where pure stoichiometric NiO undoped is an insulator material, with resistivity of the order of 10^{13} *Ω.cm* a room temperature where is classified as a Mott-Hubbard insulator.

Electronic conduction in undoped NiO is suggested to the appearance of nickel vacancies or excess of oxygen. In the ionic crystal of NiO, the radius of O^{2-} (0.140 nm) is superior to that of Ni^{2+} (0.069 nm) consequently overload of O in NiO create vacancies in the normally occupied Ni sites. However, to conserve global electrical neutrality in the crystal, two Ni^{2+} ions should be converted to Ni^{3+} for every vacant Ni^{2+} site, whither the Ni^{3+} ions play a positive center for electron hops from a Ni^{2+} to a Ni^{3+} site, it looks as if there is a positive hole moving around the Ni^{2+} sites.

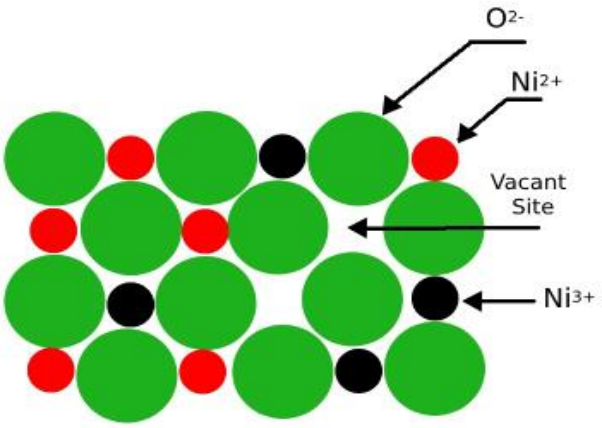

Figure I.3. A pure non-stoichiometric NiO crystal schematic.

I.2.1.4 Magnetic Properties:

NiO is an important transition metal oxide which has been of interest due to its interesting magnetic properties. Any change in the structure of crystal with temperature in fact it's linked with the magnetic properties of NiO. Néel temperature (TN) is the temperature at which antiferromagnetism changes to paramagnetism. Above the Néel temperature TN = 523 K, nickel oxide crystallized in a cubic rock-salt crystal structure (group Fm-3m) and exhibit paramagnetic behavior whereas, below Néel temperature TN and at room temperature, nickel oxide crystallized in rhombohedral structure (group R3m) which is a Mott insulator shows antiferromagnetic behavior, the magnetic structure of NiO consists of ferromagnetic sheets of Ni^{2+} parallel to the {111} planes with opposite spin directions in neighboring sheets, and the structure of NiO undergoes a week cubic-to-rhombohedral distortion due to the magnetostriction effect [42-45].

The magnetic properties of NiO, furthermore to depending on transition metal (TM) ion doping, as nanoparticles magnetic properties can differ from the bulk magnetic structure, because of the influence of surface effects [46], whereas magnetic properties sensitively depend on the size of the particles in nanoscale. When the dimension is minimized to nanoscale, the NiO is shown to exhibit various magnetic properties as ferromagnetism (size of particles, $D \leq 24$ nm) [47], superparamagnetism ($D \leq 31.5$ nm) [48], behavior of spin glass ($D \leq 10$ nm) [49-50].

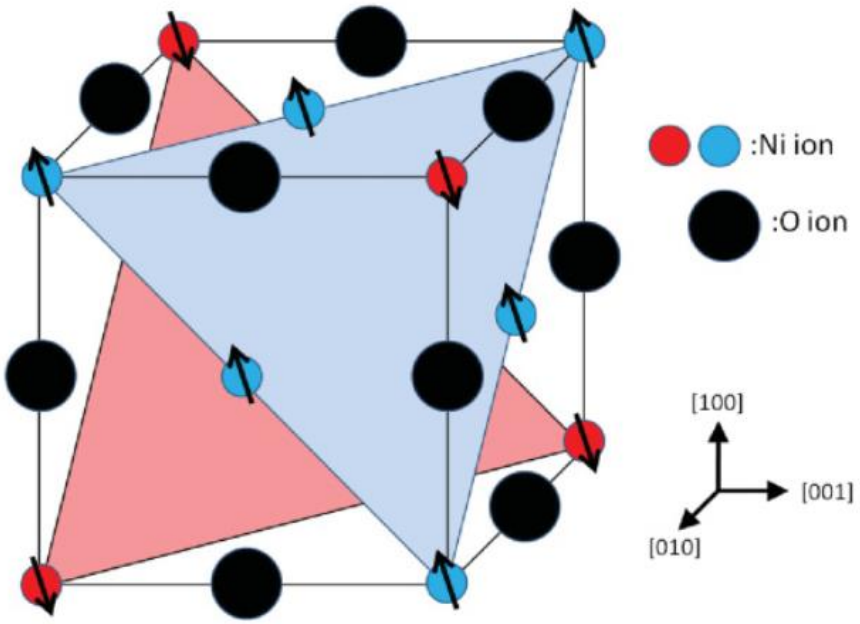

Figure I.4. Schematic illustration of the antiferromagnetism spin structure in NiO. The spins couple ferromagnetically within the same {111} planes [51].

I.3 Latest work and applications on nickel oxide thin films:

The versatility of NiO thin films makes them valuable materials for a wide range of applications due to their excellent durability, chemical and thermal stability, controllable conductivity with high transparency, low cost and catalytic properties. Additionally, NiO is quite compatible to be incorporated with the wide range of n-type TCOs due to its rock salt structure resulting in ease of lattice matching [52].

I.3.1 Transparent Electrodes for Flexible Organic Photovoltaic Cells:

Transparent electrodes with a dielectric−metal−dielectric (DMD) structure can be implemented in a simple manufacturing process and have good optical and electrical properties. Nickel oxide (NiO) introduced into the DMD structure as a more appropriate dielectric material that has a high conduction band for electron blocking and a low valence band for efficient hole transport. The indium-free NiO/Ag/NiO (NAN) transparent electrode exhibits an adjustable high transmittance of ~82% combined with a low sheet resistance of ~7.6 $\Omega \cdot s \cdot q^{-1}$ and a work function of 5.3 eV. The NiO/Ag/NiO electrode shows excellent surface morphology and good thermal, humidity, and environmental stabilities [53].

Organic photovoltaic (OPV) cells have unique properties including low weight, flexibility, low cost, and suitability for large-scale production, making them very attractive as a renewable energy source. Although their power conversion efficiency (PCE) has reached over 9% with recent rapid progress in OPV technology and interfacial materials [54-55]. The power conversion efficiencies of organic photovoltaic cells with NAN electrodes deposited on glass and polyethylene terephthalate (PET) substrates are 6.07 and 5.55%, respectively, which are competitive with those of indium tin oxide (ITO)-based devices [53].

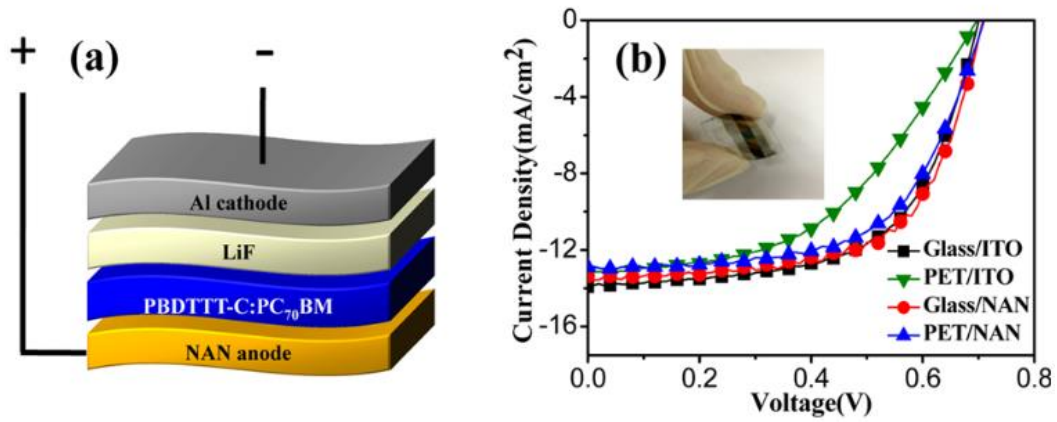

Figure I.5. (a) Configuration of the OPV based on the NAN electrode. (b) J−V characteristics of the OPVs based on ITO and NAN electrodes on glass and PET substrates [53].

I.3.2 Thin Film Transistors (TFTs) :

Oxide-based thin-film transistors (TFTs) have been extensively investigated for emerging applications of the next generation active-matrix liquid crystal displays, organic light emitting diode displays and other electronic circuits [56-57]. The challenge is to develop complementary circuits using oxide semiconductors. However, both n-type and p-type transistors are required to realize complementary circuits. NiO is a semi-transparent, interesting Mott insulator with a wide bandgap of 3.7 eV. Oxygen-rich non-stoichiometric NiO films become fairly good p-type semiconductor. Due to its excellent chemical stability, magnetic, electric and optical properties and low cost, the NiO films are regarded as an attractive p-type oxide semiconductor for optoelectronics applications [58-59].

Oxide p-type transistors are expected in realization of complementary circuits. Recently, amorphous p-type NiO thin films deposited on glass substrates various O_2/Ar flow ratios. Pure Ar ambient with room temperature (RT) growth of NiO films shows the highest mobility of 1.07 cm^2/Vs, and hole concentration of 2.78×10^{17} cm^{-3}. Initial p-type NiO-based thin film transistors grown by magnetron sputtering demonstrated a mobility of 0.05 cm^2/Vs, a threshold voltage (V_{th}) of −8.6 V, subthreshold swing (S) of 2.6 V/dec, the current on–off ratio of 10^3, respectively [60].

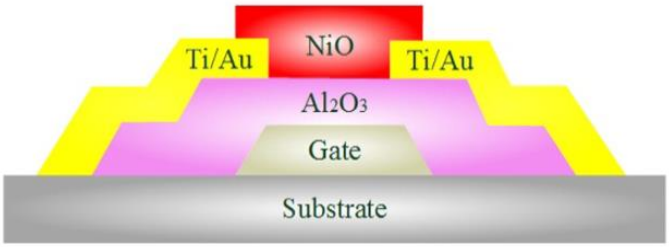

Figure I.6. The schematic diagram of the NiO-based TFT [60].

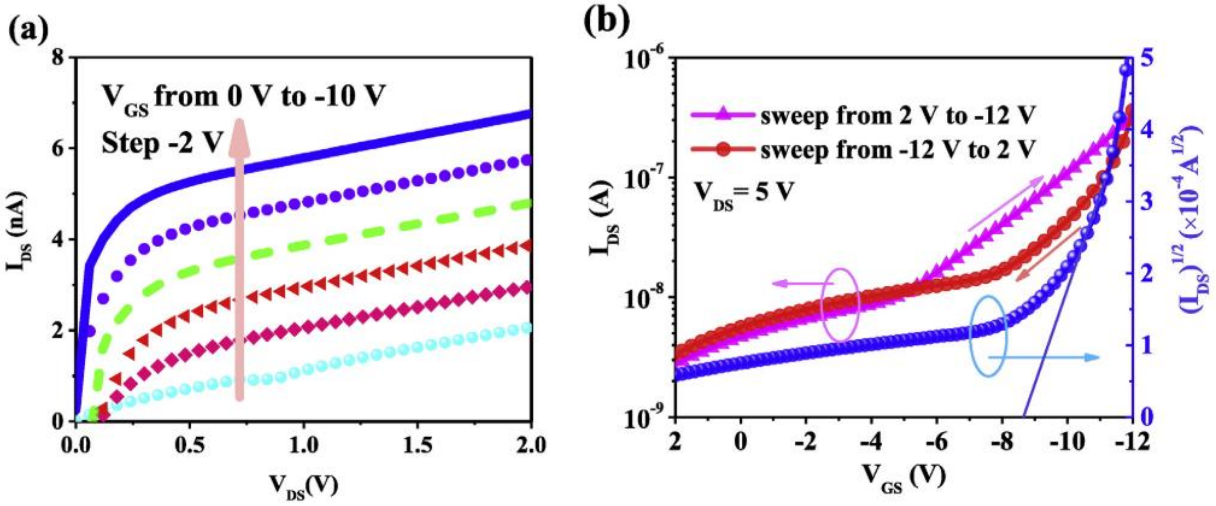

Figure I.7. (a) IDS–VDS characteristics of the NiO TFTs with Al_2O_3 gate dielectric insulator. (b) IDS–VGS characteristics of the NiO TFTs with Al_2O_3 gate dielectric insulator [60].

I.3.3 Organic Light-Emitting Diodes (OLEDs):

The OLEDs are thin film devices which consists in principle organic emitting layer and hole transporting layer integrated between anode and cathode electrodes. The bottom electrode is high transparency thin film deposited onto suitable transparent substrate whereas the top electrode is generally highly reflecting. The voltage is applied between anode and cathode electrodes where the holes are injected from cathode and electrons from the anode electrode by the electric current. The injected charges come together and recombine in emissive layer. Photons are created, so light is emitted, in a frequency corresponding to the energy gap between conduction band and valence band of this emissive layer.

Highly efficient OLEDs are generally fabricated using thermal evaporation, but this technique has some restrictions in manufacturing such as high processing cost and lack of ability to deposit onto large areas. On the other hand, solution-processed OLEDs offer low cost and large area applications on flexible substrates. Although, low efficiency is often a problem for solution-based processing, this challenge can be eliminated by charge blocking layers. However, solution-based techniques limit the deposition of multilayer structures due to dissolving or damaging the subsequent layer by its solvent [61].

There are many reports on solution-processed nickel oxides (s-NiO_x) are used as hole injection and transport layers in solution-processed organic light-emitting diodes (OLEDs). By increasing the annealing temperature, the nickel acetate precursor fully decomposes and the s-NiO_x film shows larger crystalline grain sizes, which lead to better hole injection and transport properties. With a p-type thin film transistor (TFT) configuration, the high-temperature annealed s- NiO_x film shows a hole mobility of 0.141 $cm^2 V^{-1} s^{-1}$, which is significantly higher compared to conventional organic hole transport layers (HTLs). Due to its improved hole injection and transport properties, the solution-processed phosphorescent green OLEDs with NiO_x HIL/HTL show a maximum power efficiency of 75.5 ± 1.8 lm W^{-1}, which is 74.6 ± 2.1 % higher than the device with PEDOT:PSS HIL. The device with NiOx HIL/HTL also shows a better shelf stability than the device with PEDOT:PSS HIL. The NiO_x HIL/HTL is further compared with PEDOT: PSS HIL/N, N’-Di(1-naphthyl)-N, N’-diphenyl-(1,1’- biphenyl)-4,4’-diamine (NPB) HTL in the thermal-evaporated OLEDs. The device with NiO_x HIL/HTL shows a comparable efficiency at high electro-luminescence (EL) intensities [62].

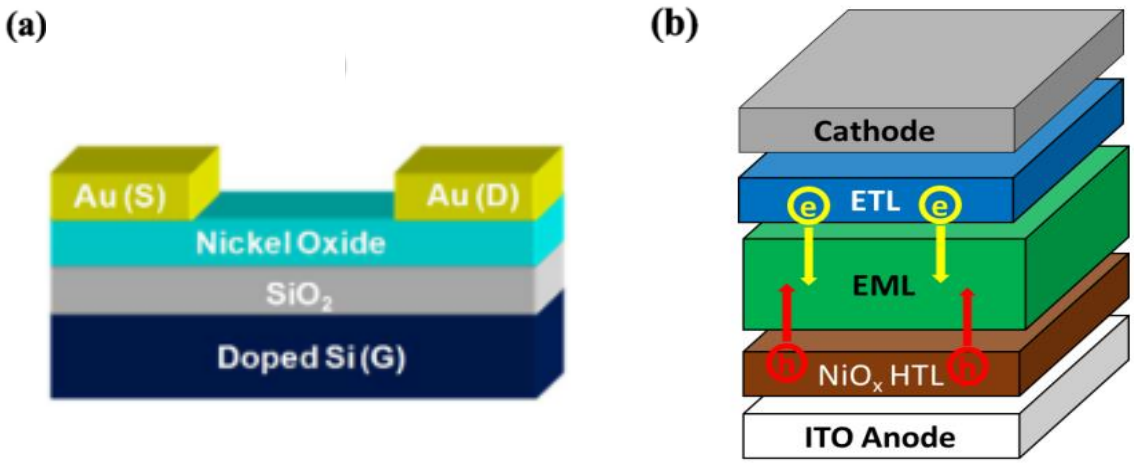

Figure I.8. (a) The structure of s-NiO_x thin film transistor, (b) The schematic cross-section of OLED [62].

I.3.4 Electrochromic Devices (ECDs):

The electrochromic devices (ECDs) or cells considered as rechargeable thin film batteries whereas ITO thin films are mostly preferred materials coated on substrate as a transparent conductive electrode. The ECDs including smart windows can modulate transmitted/reflected visible electromagnetic waves. The ECDs generic structure is a substrate coated with a TCO material, the electrochromic coating, an electrolyte, an ion reservoir, an additional conductor and again a substrate [63-64], where TCO behaves as the electrode which provides the connection of device and external battery. The electrochromic material deposited onto TCO substrate to investigate the contact between electrochromic film and ion conductive electrolyte hose other side is in contact with ion reservoir.

The voltage applied throughout electrolyte-substrate coated with TCO film where the electrical current drives the ions from reservoir into the electrochromic film over the electrolyte and injects the electrons from the conductive coating of the substrate.

The optical characteristic of electrochromic layer is altered by the injected electrons due to their tendency to charge neutrality. The reverse voltage ejects the ions out from the reservoir while the electrons leave through the substrate, therefore, electrochromic material is converted to its original state.

The electrochromic materials are divided into three classes:

- The electrochromic materials are colored in both oxidized and reduced states
- Cathodically coloring materials: These are colored in the reduced state and colorless in the oxidized state.
- Anodically coloring materials: These are colored in the oxidized state and colorless in the reduced state.

The electrochromic NiO is an anodically coloring inorganic material. In oxidized state, the color of NiO turns to dark bronze [63]. A several studies has been recently reported on NiO as a counter electrode for NiO/ WO_3 electrochromic applications [65-66].

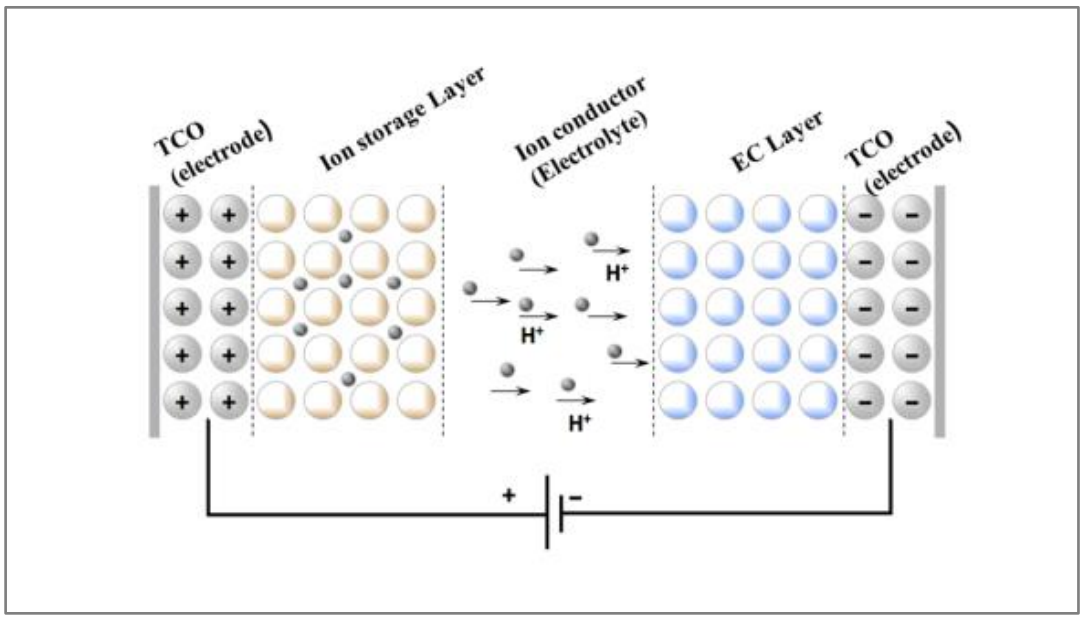

Figure I.9. The basic structure of Electrochromic Devices ECDs [65].

Ongoing research and development continue to explore new works and applications to improve the performance of NiO thin films making them useful for various purposes.

I.4 Nickel oxide doping:

Mastery of both types of doping n and p is necessary to create a p-n junction which can then partially or totally compensate each other. The interest is to obtain a semiconductor with greater physical properties. To improve the conductivity, magnetic, optical and other properties of materials require an increase in the number of charge carriers, which is achieved by doping. Depending on the nature of the doping, the type of conductivity and the properties of the materials can change. Doping can lead to p-type or n-type conductivity, depending on the nature of the doping element [67].

The n-type doping is defined by the substitution of a few nickels or oxygen atoms by other atoms. Ni can be substituted by group 3 elements such as Ga, In and Al [68-70]. These have a greater number of free valence electrons than nickel, and have an extra electron compared with the initial ion (Ni^{2+}). The initial covalent bonds are restored, but one of the electrons remains free. The inserted ion is said to be an electron donor. To obtain the same result, some oxygens can be replaced by group 5 elements such as chlorine (Cl) or iodine (I) [71].

The p-type doping is based on replacing a few nickel atoms with group I elements such as lithium, potassium or sodium, which contains fewer free electrons compared to nickel. A peripheral electron is then missing to re-establish all the initial covalent bonds. This results in the appearance of a hole giving the inserted atom the character of an electron acceptor, as it is capable of receiving an additional electron. These atoms can also occupy interstitial sites acting as a donor (they have one or more free electrons in the conduction band) and not as an acceptor. In addition, oxygen atoms can be substituted by a group V element (P, As or N...) which will act as an electron acceptor. The latter can substitute not only oxygen but also nickel atoms, which could make them donors.

I.4.1 Lanthanum material:

Lanthanum (La) is a chemical element with atomic number 57 and melting point among them: 920 °C. It is a soft, ductile, silvery-white transition metal where is traditionally counted among the rare earth elements. The 57 electrons of a lanthanum atom are arranged in the complex electronic configurations $[Xe]5d^16s^2$ were involving partially filled 4f or 5f orbitals with three valence electrons outside the noble gas core. Lanthanum almost always gives up these three valence electrons from the 5d and 6s subshells to form the +3-oxidation state, were ionic radius of La^{3+} is greater than that of Ni^{2+} [72-73].

Table I.2. Room-temperature properties of lanthanum element (La) [74].

Properties:	$_{57}$**La** − ($_{54}$**Xe core**) + **4f** ^{0} + **6s**^{2} **5d**^{1}	$_{57}$**La**
Valence		**+3**
Density (g/cm^{3})		**6.15**
Melting temperature (◦C)		**918**
Thermal conductivity (W/m·K)		**13.4**
Elastic (Young's) modulus (GPa)		**36.6**
Coefficient of thermal expansion (10^{-6} m/m·◦C)		**12.1**
Electrical resistivity (μ.cm)		**61.5**
Ionic radii (pm)		**117.2**

I.4.2 Lanthanum doped nickel oxide (LNO):

Recently, La-doped NiO have attracted much attention for interesting applications, the introduction of La into the NiO lattice generate changes in electronic configurations and consequently affect the material properties, making it an effective dopant for adapting NiO characteristics. Due to La unique electronic structure and large ionic radius, its incorporation into the NiO lattice may affect key properties such as electrical conductivity, charge carrier mobility [75]. From many literatures, it is reported that the use La doping considerably enhances NiO's optical absorbance making it ideal for a wide range of optoelectronic uses [76]. When La was applied as doping element, more surface defects are occurred, which hindered the recombination of photo-induced electron-hole pairs, were this contributed to the improvement of the photocatalytic activity.

However, a comprehensive understanding of the synthesis methods and their influence on the optical characteristics of La-NiO thin films remains inadequate and demands more investigations. These characteristics make (LNO) a technologically important and enables researchers to customize and improve material for particular uses, improving solar cell efficiency, maximizing the performance of photo-electrochemical cells, and raising the sensitivity of gas sensors [77].

I.5 Thin film concepts:

Thin films (TFs) are often describing a layers of material atoms can vary from a few atomic layers to around ten micrometers. These coatings modify the properties of the substrate on which they are deposited. Since TFs are nano-objects in one direction in space, the physical and chemical properties of thin films can differ from those of macroscopic objects in all their dimensions, depends on the methods and conditions of their preparation, such as changing the type or percentage of impurities added or changing the temperature of the base. The main difference between thin and thick film deposits is the thickness of the deposited layers, were the arrangement of the elements of material is in two dimensions with the thickness of the third dimension.

I.5.1 Mechanism of film formation:

The thin film deposition process can be classified into three main phases:

- Preparation of the film forming particles (atoms, molecules, cluster).
- The particles transport from the source to the substrate.
- The particles adsorption on the surface of substrate and finally growth of thin film.

These phases can be linked to the specific deposition process and/or on the selection of the deposition parameters, they can be considered either independent or influenced by each other. A thin film is prepared by deposition film materials (metals, semiconductors, insulators, dielectric etc.) atom by atom on the substrate through phase transformation. A suitable time interval is required between the two successive deposits of atoms and layers.

In thermodynamically stable films, all atoms (or molecules) will take up positions and orientations energetically are similar with neighboring atoms of the substrate or earlier deposited layers, and then the effect substrate or else first layers will diminish gradually [78].

I.5.2 Thin film growth process:

The main steps in a typical thin film deposition process are [78]:

1. Thermal accommodation,
2. Adsorption (physisorption) of atoms/molecules,
3. Diffusion in the Surface,
4. Formation of atoms- atoms and substrate- atoms bandings (chemisorption),
5. Nucleation: aggregation of single molecules /atoms,
6. Formation of structure and microstructure (single crystalline, polycrystalline, amorphous, roughness and defects, etc.),
7. Modification within the bulk of the film (diffusion, grain growth etc.).

In thin film formation there exist three mechanisms of thin film condensations which can be distinguished, depending on the strength of interaction between the growing atoms and the deposited atoms of the film in the substrate. These are:

a) The layer-by-layer growth,

b) A three-dimensional nucleation, forming, growth and coalescence of islands;

c) Absorption of monolayer and subsequent nucleation on the top of this layer.

I.5.2.1 Nucleation :

Nucleation is the birth stage of a film. Condensation is started by the production of the small cluster through the combination of numerous absorbed atoms. There are two kinds of nucleation occur during the production of a film [79]:

- Homogeneous nucleation: The total free energy is used in the formation of a cluster of adatoms
- Heterogeneous nucleation: Particular shapes of clusters formed by collisions of atoms on the surface of the substrate, and in the vapor phase its supersaturation is adequately high.

I.5.2.2 Growth modes :

The process of enlargement of the nuclei to final form a coherent is termed as growth, the growth of thin films on a substrate is classified into three categories, illustrated schematically on the Figure I.10 based on the electron microscope observations are. These modes are named after their original investigators and are as follows [80]:

- Island (**Vollmer- Weber type**) growth mode (Fig I.10.a) corresponds to the situation when film atoms are more strongly bound to each other than to the substrate. In this case, three-dimensional islands nucleate and grow directly on the substrate surface.

- Layer-by-layer (**Frank-van der Merve type**) growth mode (Fig I.10.b) refers to the case when the film atoms are more strongly bound to the substrate than to each other. As a result, each layer is fully completed before the next layer starts to grow, i.e., strictly two-dimensional growth takes place.

- Layer-plus-island (**Stmnski-Kmstanov type**) growth mode (Fig I.10.c) represents the intermediate case between FM and VW growth. After the formation of a complete two-dimensional layer, the growth of three-dimensional islands takes place. The nature and thickness of the intermediate layer depend on the particular case (for example, the layer might be a sub-monolayer surface phase or a strained film several monolayers thick).

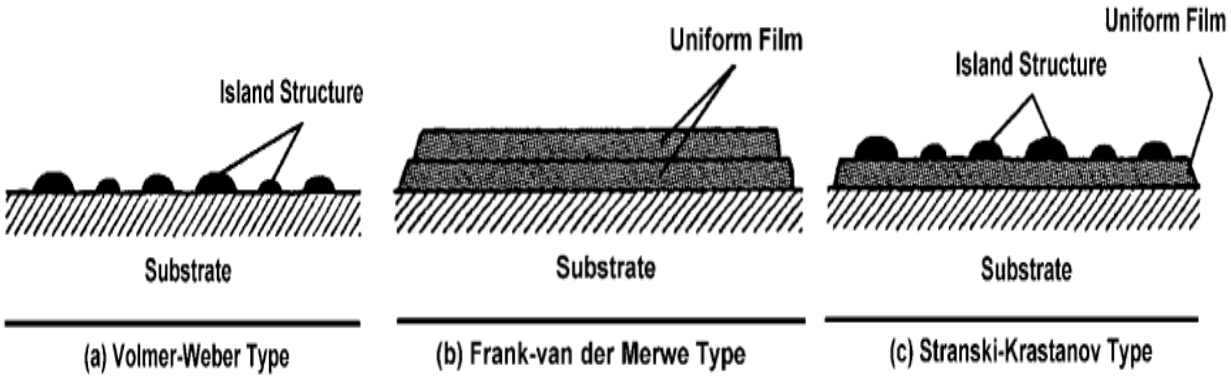

Figure I.10. Schematic representation of the three main growth modes: (a) layer-by-layer growth mode, (b) layer-plus-island growth mode, (c) Island growth mode [81].

I.5.3 Deposition techniques of thin films:

Thin films deposition methods so diverse, TFs deposition can be generally grouped into physical methods such as evaporation or sputtering, and chemical methods, vapor or liquid phase. The physical methods, notably ultra-vacuum evaporation is mainly used by research laboratories because they make it possible to develop very diverse materials and to measure physical parameters in-situ. Chemical methods, more specialized, on the other hand much more interesting for series manufacturing of industrial components when possible [82].

The broad classification of deposition techniques is outlined in the Figure I.11. An enormous number of deposition processes that exist and just only some methods are detailed in the next parts with special emphasis on the sol-gel spin-coating method [83].

In order to optimize the desired film characteristics, a good comprehension of the advantages and restrictions applicable to each technique is necessary. The choice of a specific deposition technique related to some factors, they are: the rate of deposition, limitations imposed by the substrate, adhesion of the deposits to a substrate, throwing power, the purity of target material, costs, ecological considerations and the abundance of the material to be deposited [84].

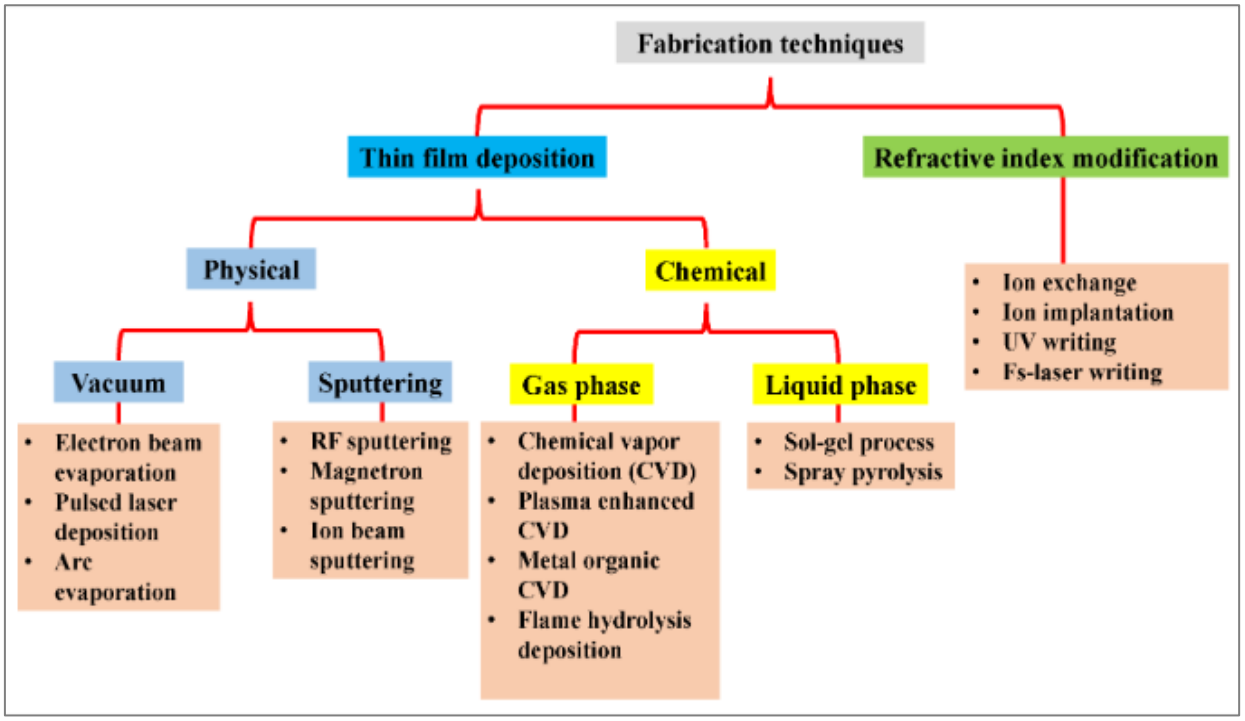

Figure I.11. A layout of most widely used techniques to fabricate TFs [82].

I.5.4 Sol-gel based coating techniques:

The sol-gel process is one of the mainly useful solution deposition methods of thin films. whose name originates as a combined short form of solution and gel, The precursor (starting material) is generally formed of the pertinent transition metal alkoxide of the form $M(OR)_n$ or $MO(OR)_n$ in water or an organic solvent. M and R here represent respectively, the metal and the alkyl group. Moreover, the solution may contain some functional additives like stabilizers that chemically improve the solution homogeneity. The liquid-filled solid network called gel is originated by the linking colloidal particles with one another in 3D structure. The transformation from solution to gel is most commonly induced by changing the pH value of the solution via catalysts such as acids and bases.

Sol-gel offers low temperature route for production of complex/functional oxide structures and deposition of sol onto complex-shaped or large surfaces [85]. It has several chemical and physical steps which are hydrolysis, condensation, drying and densification [86]. It is possible to fabricate high purity products such as micro and nano particles in different size/shape, fibers, membranes, powders and coatings by sol-gel process.

I.5.4.1 Dip coating:

Dip-coating technique is the immersion of a substrate into the coating sol and subsequently withdrawing a substrate from sol or moving the sol away from the substrate for thin film deposition. This process allows the coating a both sides of the substrate simultaneously, large scale thin film production and offers the deposition of sol onto curved or complex-shaped substrates. Dip-coating divided into these steps as follows:

- Immersion: the substrate is immersed into the coating sol at a constant rate.
- Hold time: the dipped substrate is holding in the sol for a determinate period of time to allow the penetration of sol particles
- Deposition: sol is deposited on the both sides of substrate while substrate is pulled up at a constant rate without any vibrations. Thickness of the film is dependent on this withdrawal speed such as, a thicker film is produced due to the higher speed.
- Evaporation: draining of excess amount of sol and evaporation of a solvent from the deposited film. The evaporation process has already started throughout the deposition step, if solvent is volatile, such as alcohols.

In the dip-coating process the important parameters are the molar concentration of the solution, relative humidity, duration of immersion, and withdrawal speeds, as well as the postdeposition treatment [87]. Viscosity and density of sol and withdrawing speed of a substrate are determinants of the film thickness.

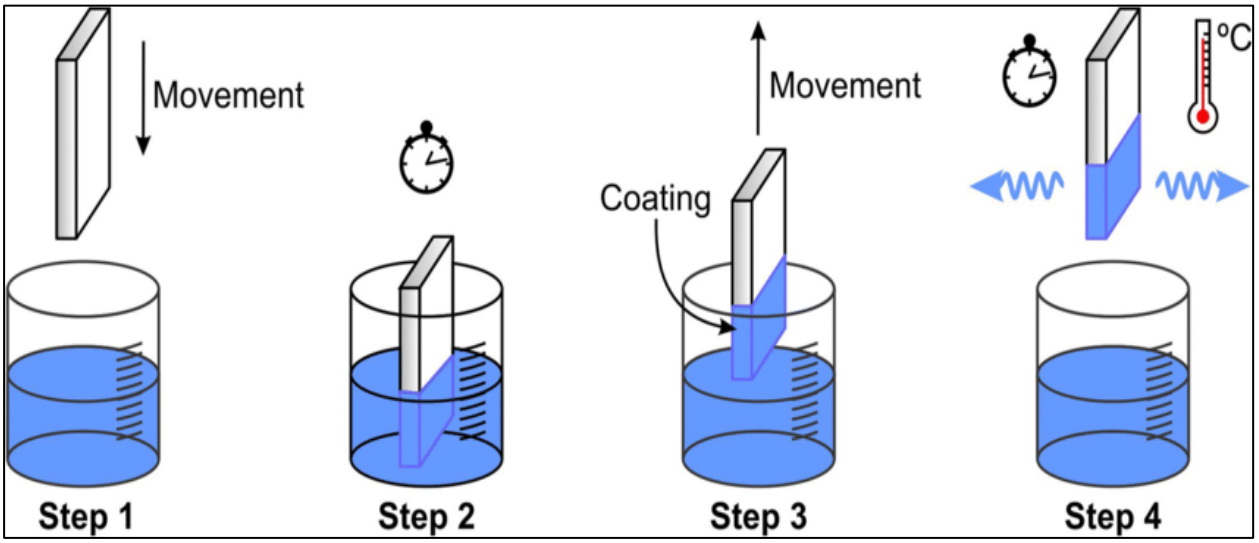

Figure I.12. The mechanism of dip-coating process [88].

I.5.4.2 Spin coating:

Spin-coating is widespread practice to obtain quite dense and uniform thin films from few nanometers to few micrometers in thickness on flat surfaces. Spin-coating enables the production of single/multi-layered thin films quick, easy and reproducible; therefore, it is widely used in variety of industries and technological applications. However, the foremost weakness of this technique is that spin coating is applicable on flat surfaces only.

This technique is mainly based on the draining by centrifugal force and evaporation of solvent deposited thin film. In addition, the parameters of importance are molar concentration of the solution, volume of solution placed on the substrate, spinning speed, and duration, as well as the postdeposition treatment [89]. Spin-coating process is composed of these steps which are deposition, spin-up, spin-off and evaporation.

- Deposition: to get completely wet surface, substrate is coated by excess amount of sol.
- Spin-up: substrate is accelerated up to the final selected speed for desired time; therefore, by the effect of centrifugal force, sol covers all over the surface and excess is flung off.

- Spin-off: substrate starts spinning at constant speed, viscous forces lead to fluid thinning mechanism and edge effects are commonly observed due to the high spin speed.
- Evaporation: coating thinning mechanism dominates and almost all solvent evaporates simultaneously in this step of the processing; since, solvents used in composition of sol is typically volatile, such as alcohols.

The spin-coating method, however, is more advantageous for research laboratories because of the material wastage involved. It is generally suitable for uniform application of thin films over small areas.

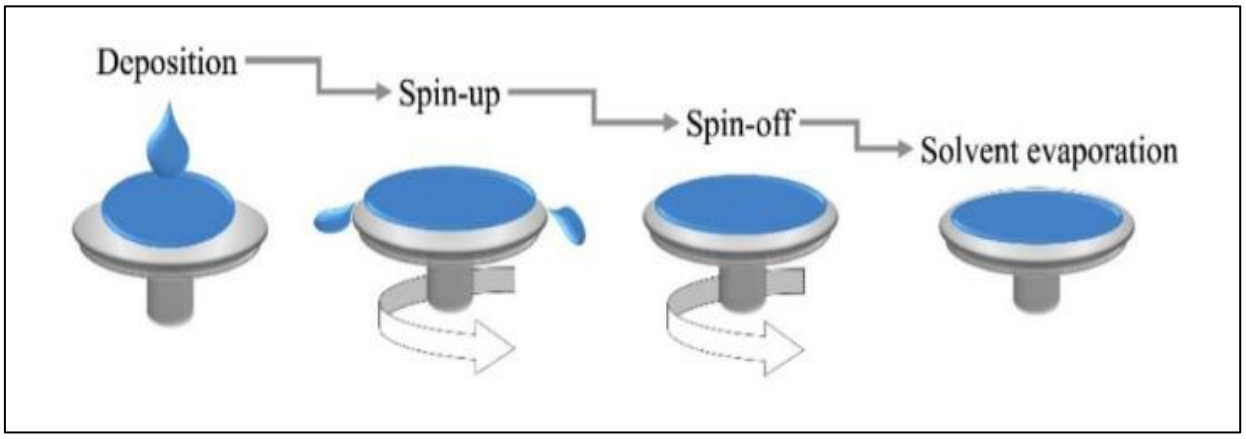

Figure I.13. The mechanism of spin-coating process [90].

Chapter II: Materials and methods

II.1 Introduction :

Nickel oxide (NiO) thin films can be prepared by different techniques and for this purpose have also been developed. Sol-gel spin-coating is the most commonly used technique adopted for the deposition of metal oxides, alloys and many compounds, this technique particularly attractive because of its simplicity, efficiency and efficacy. The enhancement of the film properties prepared with spin-coating is largely correlated with the deposition conditions parameters, which affect the physical properties. Recently, numerous researchers have been described the influences of precursors, solution concentration, temperature, solvent nature, annealing treatment and film thickness on NiO films properties [91-96]. In this chapter, we describe some of the most widely used experimental techniques for obtaining La-doped NiO thin films, using the spin-coating technique, and also its characterization techniques used to measure their optical and structural properties is discussed below.

II.2 Materials :

The list of the chemicals used in this study are given in Table II.1. All chemicals were used as supplied without any purification.

Table II.1. The list of the chemicals used in this study

Material	Nickel (II) nitrate hexahydrate	Lanthanum (III) nitrate	Ethanol
Linear formula	$Ni(NO_3)_2 \cdot 6H_2O$	$La(NO_3)_3$	C_2H_6O
Appearance	Emerald green	Colorless	Colorless
Molecular mass	290.8 g/mol	324.92 g/mol	46.068 g/mol
Physical state	Hygroscopic solid	Crystals solid	Liquid
Density	2.05 g/cm^3	1.3 g/cm^3	0.78945 g/cm^3
Melting point	56.7 °C	40 °C	−114.14 °C
Solubility in water	243 g/100ml (0 °C)	158 g/100 ml (25 °C)	Miscible

II.3 Elaboration of NiO thin films:

II.3.1 Experimental montage of spin-coating system:

Spin-coating technique produces homogeneous and uniform thin films in the thickness range of micrometer to nanometer. After mounting a substrate on the spin-coater and put a small drop of solution on it, the substrate undergoes a rotational movement, the aim of which is to obtain a homogeneous spread of the solution. Viscous force and surface tension are the main causes for the flat deposition on surface. Finally, the thin film is formed by the evaporation. Three parameters are controlled by this method:

1) Spinning speed
2) Acceleration
3) Spinning time.

Spin coating consists of several stages, such as fluid dispense, spin up, stable fluid outflow, spin off, and evaporation, respectively [97].

The advantages of spin coating are to produce very fine, thin, and uniform coating, while the disadvantage is the difficulty with large area samples [98-99]. By spin-coating method the desired thickness of the film can be achieved. Thickness of the layer depends on many different parameters, and the following equation shows how these parameters affect thickness:

$$d = \left(1 - \frac{\rho_A}{\rho_{A0}}\right).\left(\frac{3\,\eta.m}{2\,\rho_{A0}\,\omega^2}\right)^{1/3} \quad \text{(II.1)}$$

where d is thickness, ρ_A is density of volatile liquid, ρ_{A0} is initial density of volatile liquid, η is viscosity of solution, m is rate of evaporation, and ω is angular speed.

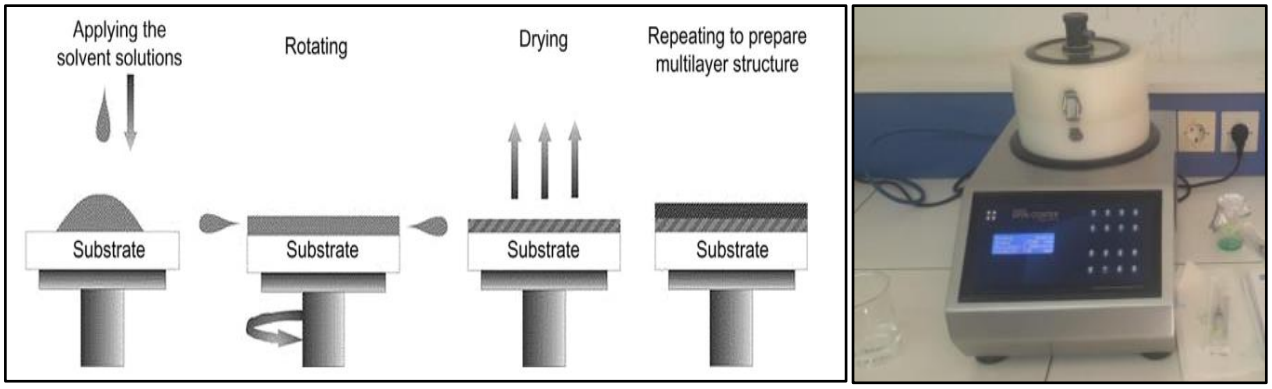

Figure II.1. Schematic of spin-coating [100], and spin-coating apparatus used in our work.

II.3.2 Experimental procedure:

II.3.2.1 Preparation and cleaning procedure of glass substrates:

The glass substrates used in this work (**R217102**), which are an optical microscope slides in size of 25×25×1 mm^3 for their availability, low price, and allowing us to study film properties, especially the optical ones. The substrates used must be clean and of good adhesion. Cleaning of substrates is a very important step to eliminate the presence of grease, dust and all other dirt and contaminations. The substrates are cleaned as follows:

1) Washes with Tap water then rinsed with distilled water.
2) Immerses slides in the HCl acid then in the acetone solution C_3H_5OH, followed by rinse with distilled water.
3) Finally, dry with a hairdryer and paper towels.

II.3.2.2 Preparation of coating solution:

In order to obtain a specific coating solution of pure and Lanthanum-doped NiO. Above all, we dissolve nickel (II) nitrate hexahydrate [Ni $(NO_3)_2$•$6H_2O$] as the precursor solution of Ni in 30 ml of ethanol solvent, and then adding a few drops of ethanolamine (C_2H_7NO) as a stabilizer at room temperature. The concentration of nickel (II) nitrate was (0.1M) and the solution mixtures were stirred thoroughly by a magnetic stirrer for 30 minutes at 60°C, leading to the formation of a clear green and homogeneous pure NiO solution. After cooling down to room temperature, solution was used for the coating process.

To calculate the mass of nickel (II) nitrate [Ni $(NO_3)_2$•$6H_2O$], the formulas II.2 is used, which gives the mass of nickel nitrate m(g) as a function of the molar mass M(g/mol), the molar concentration C(mol/L) of nickel nitrate and the volume ethanol V(L).

$$\boldsymbol{m = M * C * V} \quad \text{.....(II.2)}$$

A solution of the concentration C (0.1M) was prepared using 30 ml of ethanol and 0.8724 g of nickel (II) nitrate which was used for the coating process.

After that, we prepare the doping solution with several series, we use the same previous conditions (mass, concentration, volume), and calculate the lanthanum mass corresponding to the determine percentages (3%, 6% and 9%) using the following formulas:

$$m_{\text{Lanthanum (III) nitrate}} = x_{\text{mass}} * \left(\frac{M_{\text{Lanthanum (III) nitrate}}}{M_{\text{Nickel (II) nitrate}}}\right) * m_{\text{Nickel (II)nitrate}} * \left(\frac{M_{\text{Ni}}}{M_{\text{La}}}\right) \text{.....(II.3)}$$

Table II.2. The lanthanum mass corresponding the percentages of Ni $_{1-x}$ La$_x$ O thin films

Percentage (%) of doping	3%	6%	9%
$m_{\text{Lanthanum (III)nitrate}}$ (g)	0.0123	0.0247	0.0370

II.3.2.3 Thin film deposition parameters:

The properties of the thin film deposited by the spin-coating technique depend on several parameters belong technique as well as substrate, such as the nature and molar concentration of the precursors, the solvents used, the type of substrate, the deposition temperature, volume of the solution, duration and speed of spinning, the number of deposits (coating-drying cycle), also the post deposition heat treatment (annealing temperature) is one of the significant controllable parameters to fabricate thin films, and so on.

The aim of this work is to prepare spin-coated thin films sample series of pure NiO and La-doped NiO as a model coating, and studying the influence of Lanthanum doping concentrations on NiO properties, and we keep fixed all the other parameters related to the spin-coating process and substrate.

Table II.3. The deposition parameters of Ni $_{1-x}$ La$_x$ O thin films

Parameters	**Optimum values**
Temperature substrate (°c)	25-27
Concentration of the precursor solution (M)	0.1
Deposition time (s)	30
Deposition speed (rpm)	2500
Deposition number (times)	9
Pre-annealed temperature (°c)	240
Final annealed temperature (°c)	500

II.3.2.4 Deposition process of the NiO thin films:

Deposition of coating solution onto glass substrates by using spin coating technique, was applied at 2500 rpm for 30 s. At the end of coating step, films were dried at 240 °C for 15 min in a furnace to remove the organic compounds. In order to obtain homogeneous and dense layers, spin coating process and drying step was repeated for 9 times (coating-drying cycle). After the deposition, films were annealed at 500 °C for 2 hours under ambient conditions. The heating rate was 5 °C/min. Formation of pure and La-doped NiO films from nickel (II) nitrate hexahydrate solution involves condensation and thermal mixing with decomposition. These occur by evaporation of the solvent and surface agent during drying and also at high temperature annealing steps. It was reported that dehydration run out and decomposition was found start of nickel (II) nitrate hexahydrate above 307 °C were anhydrous Ni $(NO_3)_2$ decomposes into nitrogen oxides and NiO [101], accompanied with the decomposition of residual solvent and stabilizer. Therefore, minimum annealing temperature was determined as 400 °C. On the other hand, 500 °C was chosen as maximum annealing temperature [102]. The blueprint of production NiO thin films is given in Figure II.1.

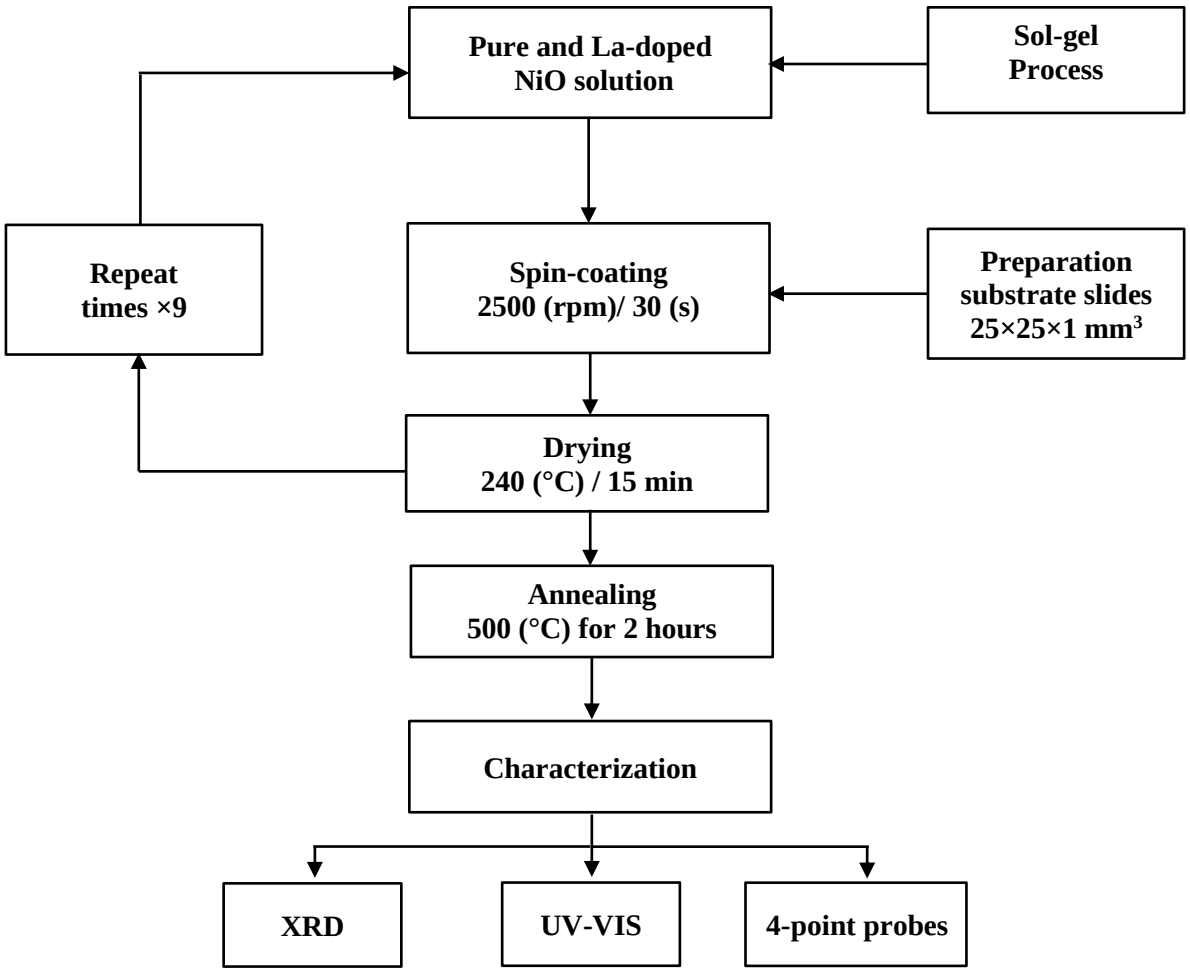

Figure II.2. Experimental procedure for fabrication of pure NiO and LNO thin films.

II.4 Characterization methods:

In order to obtain perfect and accurate films, the appropriate technology must be chosen for their preparation, and layer preview and description techniques are a key factor in knowing the features of thin films. There are many techniques available for the structural, optical and electrical characterization of thin films. We shall briefly describe the methods we have used.

II.4.1 X-ray Diffraction XRD (Structural properties):

X-ray diffraction (XRD) analyses were carried out to examine the transition from amorphous to crystalline state and identify the crystal structure of nanostructured NiO films after heat treatments. A RIGAKU MENU- FLEX 300/600 system equipped with Cu Kα radiation (alpha= 1.5406 Å) with an acceleration voltage of 40kV was used. The diffraction tests were conducted for diffraction angle (2θ) between 10° and 90° with a step of 0.03°.

II.4.2 UV-Vis Spectrophotometry (Optical properties):

UV-Vis light transmission of the film samples was recorded within the wavelength range of 300 to 1100 nm using PerkinElmer Lambda 25 UV-Vis spectrophotometer (190-1100 nm) and air measurements were taken as a background. According to the optical transmission and absorption spectra of the films, the absorption coefficient, extinction coefficient, urbach energy, optical band gaps and refractive index of the films were estimated.

II.4.3 Four-point probes (Electrical properties):

Resistivity measurements of thin film samples which represents the inverse of conductivity, were performed by four probe method using JANDEL RM 3000 source measure unit to examine the electrical conduction mechanism of the films. The measurements were carried out at ambient conditions.

Chapter III: Results and Discussion

Pure and La-doped NiO thin film samples were formed on glass substrates by spin coating of sol-gel derived solutions. The film formation behavior, structural, optical and electrical properties of the films were investigated as a function of controllable processing parameter, such as lanthanum doping concentration. This chapter starts with the structural and optical properties of thin film samples and continues on investigation of electrical properties.

III.1 Structural properties of $Ni_{1-x}La_xO$ thin films:

III.1.1 XRD analyses of $Ni_{1-x}La_xO$ samples:

Phase analyses of pure and La-doped NiO thin films annealed at 500 °C were performed by using x-ray diffractometer with diffraction angles from 10° to 90° to determine the crystal structure and evaluate the crystallinity of the films. The analyses confirmed the formation of crystalline pure and LNO thin films after annealing. The XRD pattern of these films is depicted in Figure III.1 which revealed the four peaks of different intensities as identified (111), (200), (220) and (222) in pure sample confirming the face-centered (FCC) cubic crystallin (*Fm3m* group), where the pattern is appropriately matched with the standard XRD spectrum documented in JCPDS card No. 040-835. Also, there are no peaks related to other phases such as lanthanum oxide (La_2O_3) or lanthanum nickel oxide ($LaNiO_3$) in these XRD spectra which is probably related to low La content ([La]/[Ni]) or may be due to the method of preparation and deposition of material.

The dominant peak intensity corresponding (111) orientation at 37.415° is seen at pure NiO substrate were (111) is the preferential orientation and the most encountered, thereby indicating strong orientation and good crystallinity. The peak (222) intensity not detected by XRD in all LNO samples, as well at 9 % La-NiO there is a deduction peak intensity (220), the diffraction peak steadily decreases. Peak intensity is affected by lanthanum doping, it can be seen in the figure that the intensity of XRD peaks systematically reduce with increasing La content, which signifies the increase in full width at half maximum β (FWHM).

Lattice calculations for all samples on the (111) plane were carried out using equation (III.1) and are presented in Table III.1:

$$a = d\sqrt{h^2 + k^2 + l^2} = \frac{\lambda}{2.\sin(\theta_{hkl})}\sqrt{h^2 + k^2 + l^2} \quad \text{.....(III.1)}$$

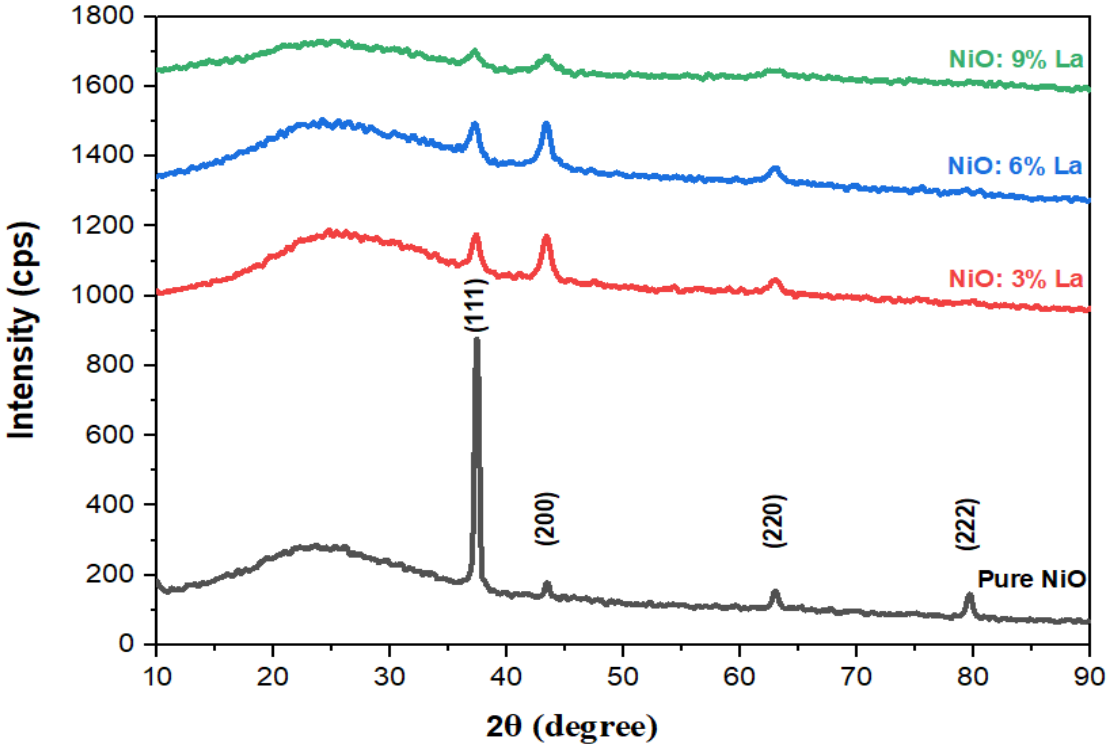

Figure III.1. XRD patterns of pure and different concentrations of La-doped NiO thin films.

The estimated data reveals a systematic expansion of the unit cell and, consequently, of its volume. This might be due to the ionic radii of 6-coordinated La^{3+} substituting for 6-cordinated Ni^{2+} in the NiO system. In general, a high ionic radii dopant will distort the crystal lattice of host materials. Therefore, La doping strongly affects lattice values, and it is expected to influence microstructural constraints like crystallite size (*D*), dislocations density (δ), and micro-strain (ε) values. The estimations of these were conducted through equations (III.2–III.4) [103–108]:

$$D = \frac{k.\lambda}{\beta.\cos(\theta)} \quad \text{(III.2)}$$

$$\varepsilon = \frac{\beta}{4.\tan(\theta)} \quad \text{(III.3)}$$

$$\delta = \frac{1}{D^2} \quad \text{(III.4)}$$

The crystallite size *D* has been determined using Sherrer formula (III.2) where λ=1.5406 (Å) is the x-ray wavelength, β is the FWHM (Full Width at Half Maximum) intensity of the main peak observed at 2θ in radian, θ is the Bragg's angle of diffraction, and *k*=0.94 is a constant.

Table III.1. Lattice parameters of pure and La-doped NiO thin films

Samples La-NiO	Peak position (111) 2Θ (°)	d_{111} (Å)	Lattice constant a_{111} (Å)	FWHM β (deg)	Crystallite size D (nm)	Micro-strain ε ($\times 10^{-3}$)	Dislocation density δ (line/cm^2) $\times 10^{12}$
0%	37.415	2.4017	4.1599	0.3280	26.7063	4.2264	0.14021
3%	37.283	2.4099	4.1741	0.9904	8.8449	12.8102	1.27823
6%	37.139	2.4189	4.1897	1.3160	6.6511	17.0925	2.26052
9%	37.121	2.4200	4.1916	1.5700	5.5750	20.4021	3.21749

In comparison with pure NiO and for La-doped NiO thin films, it can be seen that the lattice constant (a_{111}) increases with La content. This may be attributed to the difference between ionic radius of Ni^{2+} (70 pm) and La^{3+} (117 pm), which leads to an internal stress in the host lattice and affects the crystalline nature of films and then promotes the formation of defects (dislocation) in these prepared thin films.

The Figure III.2 depicts the Variations of *D*, δ, and ε values for the (111) crystallographic orientation for all samples according to La concentration. The crystallite size *D* are dramatically reduced from 26 to 5 nm with increasing La content in the NiO system. The growth in size is directly related to the dislocation density δ and micro-strain ε values, which are systematically increasing. The increases of δ and ε clearly signify the increase of defects in the system from La doping. The presence of defects due to doping will affect the optical and electrical properties of prepared thin films. Especially, the dislocations play an important role in the variation of the electrical resistance of the films.

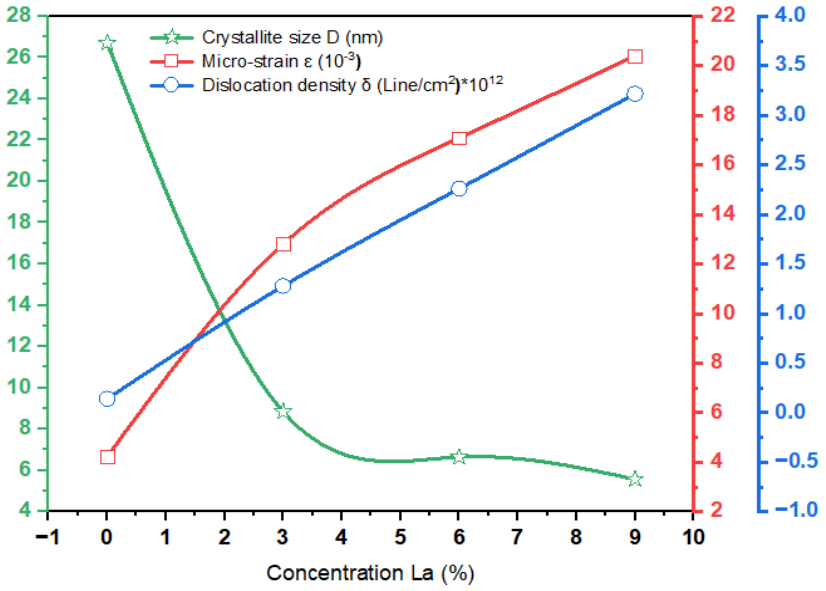

Figure III.2. Correlation between crystallite size *D*, micro-structure ε and dislocation density δ at different concentrations of La.

[36]

Crystallite size *D* generally considered to be the cubic root of the volume of a crystallite, often matches grain size but there are exceptions (different than particle size), more crystallinity means higher degree of structural ordering (atomic ordering).

Figure III.3 shows that the crystallite size *D* of samples diffraction peaks along the (111) plan decreases with increasing lanthanum concentration, although FWHM β (Scherrer's formula) increases, it is seen from that the crystallite size *D* inversely proportional to FWHM β, when crystallite size *D* gets smaller the peak gets broader, otherwise smaller FWHM β means more sharp peak more is crystallite dimension, this may be attributed to the increment of the defects and empty spaces in the crystalline structure as crystallite size decreases.

This shows that doping with lanthanum inhibits the growth of crystallites and then leading to a depressed crystallinity phenomenon. Furthermore, the decrease in the grain size with doping can improve the performance of many nickel oxide-based devices such as dye sensitized solar cells.

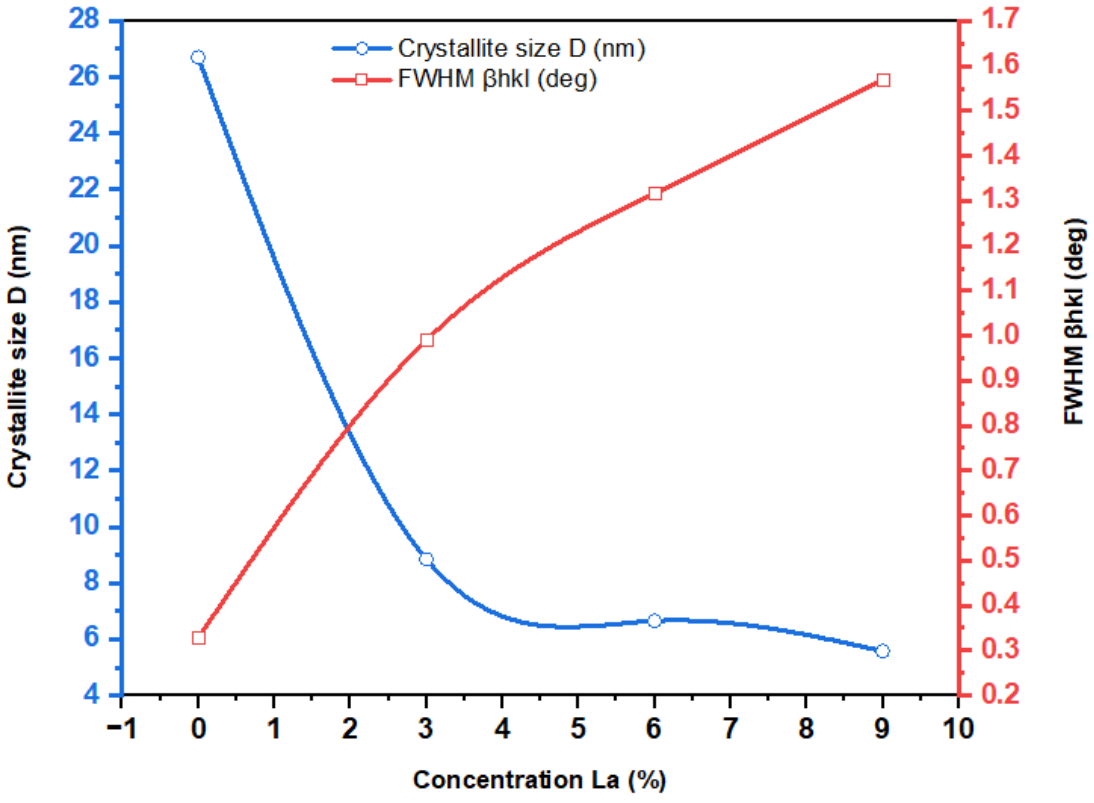

Figure III.3. Variations of FWHM β and crystallite size *D* of La-NiO films at different concentrations of La.

III.2 Optical properties of $Ni_{1-x}La_xO$ thin films:

III.2.1 Transmittance, absorbance and reflectance spectra of $Ni_{1-x}La_xO$ samples:

As the thin films prepared to achieve optoelectronic characteristics, it is necessary to study the optical properties, the important optical properties transmittance, absorbance and reflectance. The spectra of the latter properties which belongs La-doped NiO thin film samples (0 to 9 %) recorded in the wavelength range from 300 to 1100 nm annealed at 500°C are shown in Figure III.4, it can be observed the absence of interference fringes, moreover the similar behaviour of the curves confirms the uniformity of the films.

The resulting films illustrate low transparency in the ultraviolet and visible regions where the maximum average transmittance is less than 35 % recorded by 3% La-doped NiO sample, except the pure NiO thin film exhibit an average optical transparency 73% in the visible region and a highly transmittance value 83% in the range from 890 to 913 nm wavelength. The transparency decreases with increase in percentage of La-doping NiO films where the growth of the grains in the films increases with La-doping concentration, it is understood that the growth inhibits transmittance. The increased scattering and the surface roughness of samples may also be the reason for decreased transmittance of the doped films.

The samples film exhibits a strong absorbances values in the ultraviolet range corresponding to the onset fundamental absorption edge of NiO, this may be understood as the electrons absorb the light incident on it and jump to the conduction band which is termed as photo-excitation of electrons [109], while in the visible range the films show low values where the absorbance increases with increase in percentage of La-doping NiO.

Comparable to absorbance, the films possess highly and stable reflectance in the visible region where all the doped samples show 29% reflectance value, while the pure NiO is 28%. However, in the ultraviolet region a reflectance values of all samples increase sharply. It can be seen that the reflectance decreases with increase in percentage of La in the low wavelength region.

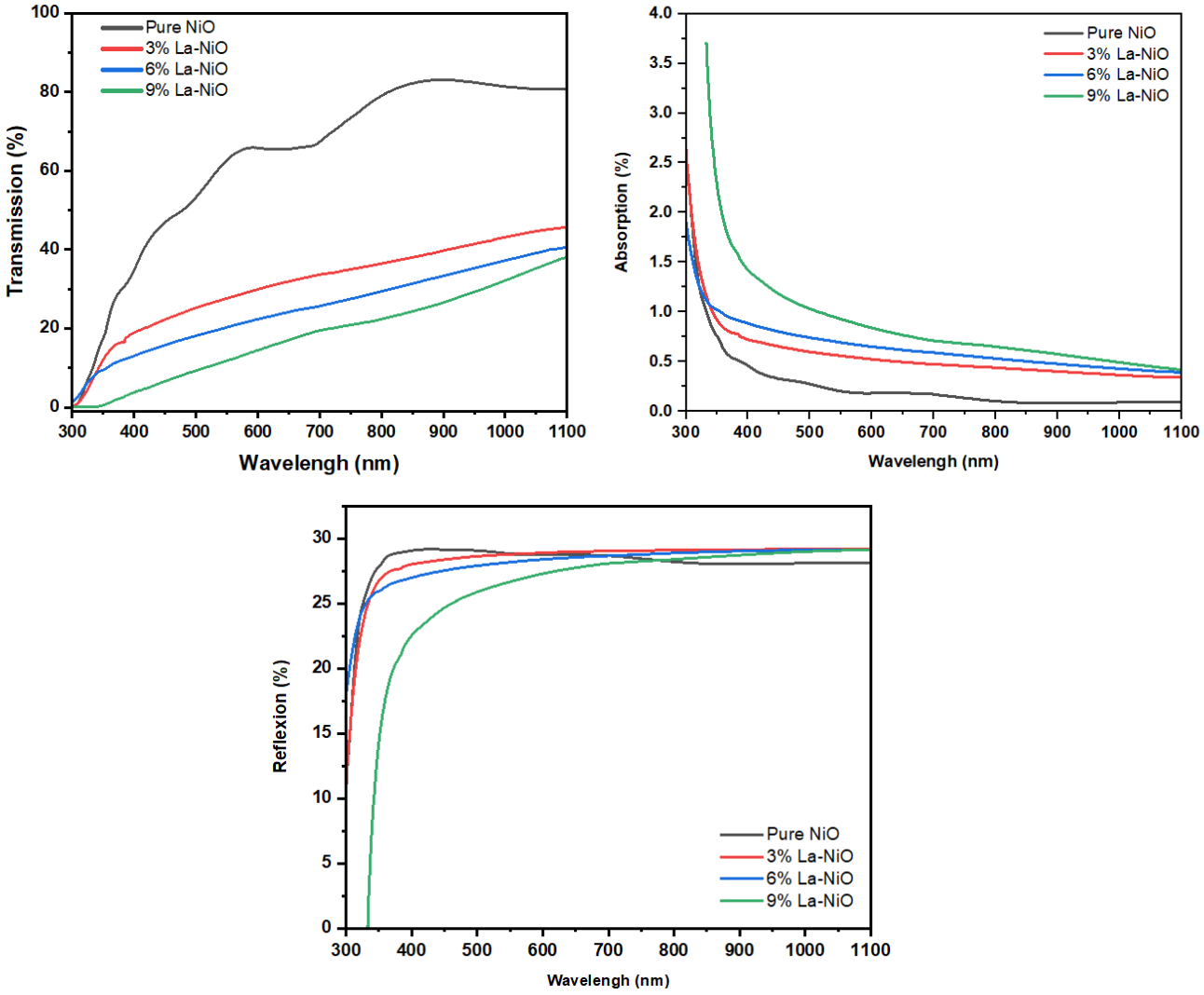

Figure III.4. Transmittance, absorbance and reflectance curves of La-doped NiO thin films according to wavelength.

III.2.2 The optical band gap (Eg) of $Ni_{1-x}La_xO$ films:

The optical absorption study was used to determine the optical band gap of thin films, which is the most familiar and simplest method. The steep falling absorbance edge indicates the semiconductor nature of the films and the optical band gap connecting absorption coefficient α of the films is obtained from the Tauc's relation [110]:

$$\alpha h\nu = B(h\nu - Eg)^n \quad \text{(III.5)}$$

where B is constant, hυ is the energy of incident photon, Eg is the energy band gap (eV) while the exponent n depends on the type of transition (n= 2 for indirect allowed, n= $\frac{3}{2}$ for direct forbidden and n= $\frac{1}{2}$ for direct allowed transitions).

The optical band gap values have been determined by extrapolating the linear portion of the curve to meet the energy axis (hν).

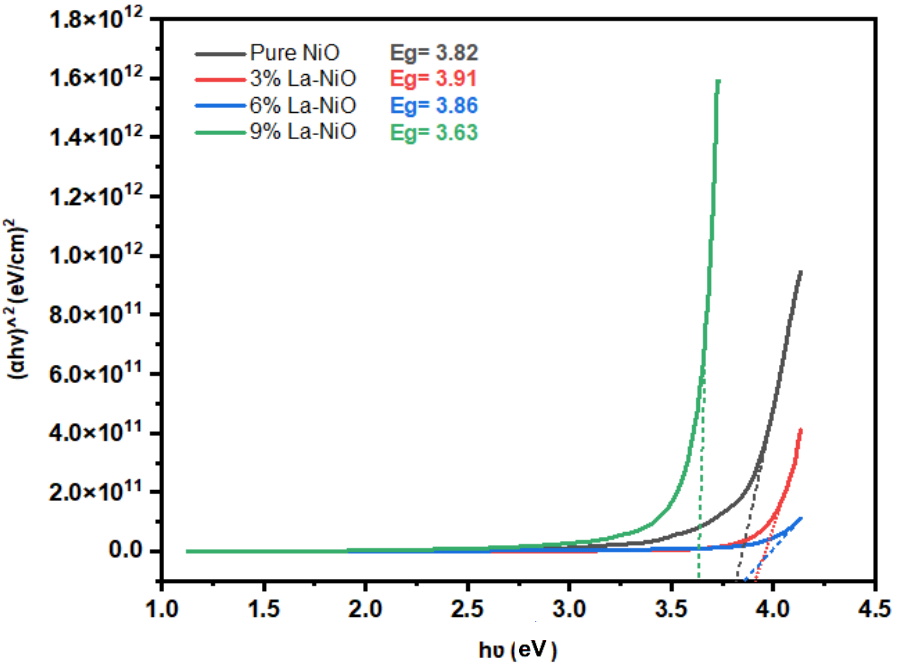

Figure III.5. Estimation of the optical band gap energy (Eg) from Tauc's relation of a direct bang gap semiconductor NiO at a different concentration La (%).

The optical analyses shows that Eg values of samples are changing only marginally with increased La doping concentration (%), the value of Eg correspond to 3% La-NiO concentration is observed higher than pure NiO, afterwards the Eg decrease with increasing La concentration.

The change in Eg as a function of dopant concentration where analyses show decreasing in Eg may be due to the generation of vacancies and states of energy between VB and CB by La doping in NiO system. Vacancies in the NiO lattice are linked with Ni substitution by La, which leads to a narrowing of the Eg. Also, the lattice constants (a) are increases with La content, the increase in interatomic distance will occur and so the decrease in binding forces among valence electrons and parent atoms will occur. The valence electrons will be freer on increasing the lattice constants, the lower energy will be required to make them freely moveable in CB. Consequently, the Eg will be reduced on rising the lattice constants, as Eg is inversely proportional to lattice constants [111].

III.2.3 Urbach energy Eu (Disorder Eu) :

The embedding of impurity into the semiconductor often reveals the formation of band tailing in the band gap caused by the formation of localized states. In these localized states charge carries can hop from one site to another. The band tail energy or Urbach energy Eu, which characterizes the width of the located states available in the optical band gap of the films affects the optical band gap structure and optical transitions, described by the following equations:

$$\alpha = \alpha_0 \, exp\left(\frac{h\nu}{Eu}\right) \quad \text{(III.6)}$$

$$\frac{1}{E_u} = \frac{d(Ln\,(\alpha))}{d(h\nu)} \quad \text{(III.7)}$$

where α is absorption coefficient and α0 is a constant. The Eu values are calculated from the inverse of the slop of Ln (α) versus (hν) curves Figure III.6.

Urbach energy increases as the La concentration increased. This changing is attributed to the disorder in the film due to the creation of new localized energy states near the band edges [112]. Moreover, this energy is associated with the micro-structural lattice disorder, where La ions causes an increase in disorder and defects in the NiO: La thin films.

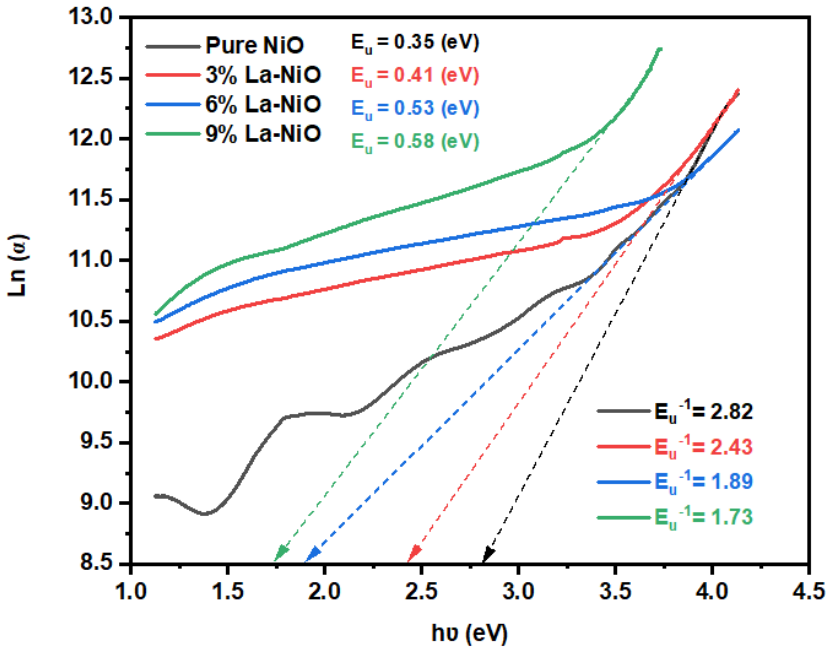

Figure III.6. Urbach energy Eu of LNO films at a different concentration La (%).

The Figure III.7 shows the variation of Urbach energy and the optical band gap Eg versus La concentration of samples, which exhibit that the both Eg and Eu values correlate very well. At first, the Eu values change similarly to the optical band gap values. But after the 6% La-NiO concentration it is clear that the optical band gap values are opposite to the disorder's variation, their values are changed inversely. As stated above, La doping produces localized states within the forbidden bad gap, as well as due to fluctuations in the density of defects and crystallite size. This behavior indicates that the obtained optical band gaps are governed essentially by the disorder variations in such films.

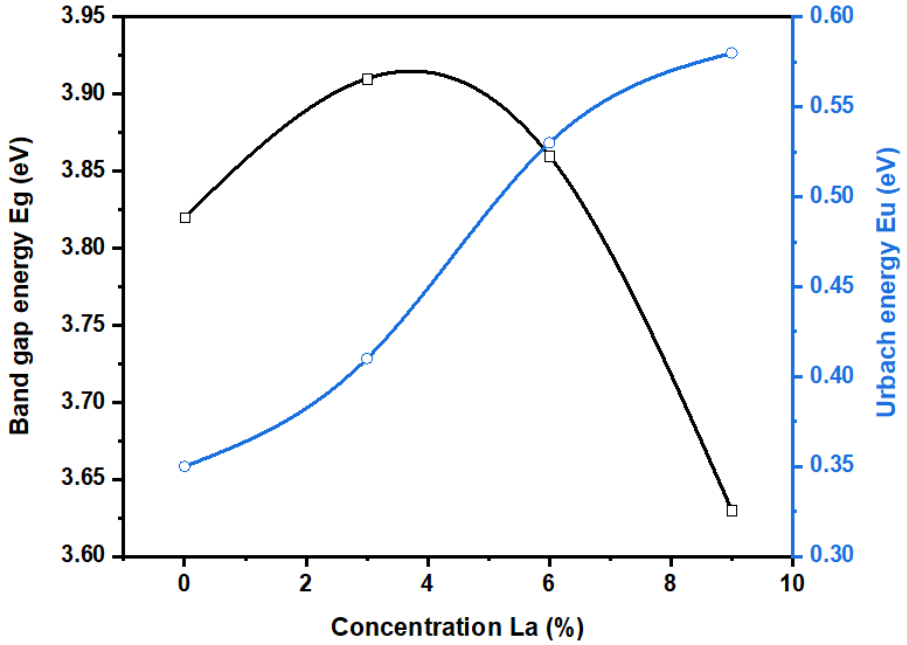

Figure III.7. The variation Urbach energy and band gap energy of NiO thin films as a function of La concentration.

III.3 Electrical properties of $Ni_{1-x}La_xO$ thin films:

NiO is an excellent insulator with a resistivity on the order of 10^{13} ∧cm at room temperature and do not show thermally induced Mott transition [113]. In this study, to carry out the resistivity measurements, the films annealed at 500 °C with different La-doping concentration were used. The four-point probe is required to measure the sheet resistance (Rs) of the films. Since negligible contact and spreading resistance are associated with the voltage probes, the sheet resistance (Rs) can be estimated, when the film thickness less than the spacing between the probes, using the following equation [114]:

$$R_s = \frac{\pi}{ln\,(2)}\left(\frac{V}{I}\right) \quad \text{(III.8)}$$

where I and V are the applied current between the outer two probes and the potential difference measured across the inner two probes respectively.

Table III.2. The calculated values of the sheet resistance Rs of La-doped NiO thin films.

La-doped NiO concentration (%)	Pure NiO	3%	6%	9%
Sheet resistance Rs (Ω/square) $\times 10^6$	2250	23.344	2.156	0.696

Table III.2 gives Rs values of the pure and La-doped NiO at room temperature, where that confirms therefore a typical semiconductor behavior in all samples. Rs value of the pure NiO thin film seems very high, it may be attributed to the low values of microstructural defects in NiO crystallites such as nickel interstitials and oxygen vacancies which implies the formation of Ni^{3+} ions in the NiO crystal which are responsible of conductivity [115-116]. Whereas Rs values of La-doped samples as can be seen that Rs decreases with an increase in La concentration, which may be due to the substitution of Ni^{2+} by La^{3+} creating more acceptor levels close to valence band edge, therefore less resistivity as La-doping level increases. This decrease is particularly important for dye solar cell applications because high electrical conductivity reduces series resistance of the cell.

The curve of Fig III.8 show that the electrical conductivity of La-doped samples was found to be in the range of 0.18×10^{-3} to $57.471\ \times10^{-3}(\Omega.cm)^{-1}$, the conductivity increases with La content where lanthanum incorporation into the film, some La^{+3} ions substitute Ni^{+2} in NiO matrix. This may be compensating the deficiencies and therefore increases considerably the electrical conductivity.

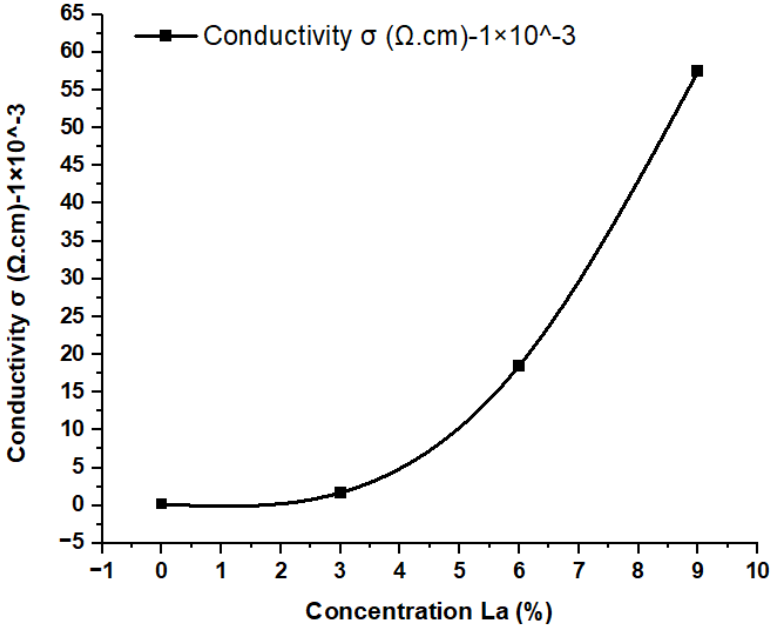

Figure III.8. The conductivity of NiO thin films as a function of La concentration.

General Conclusion

General Conclusion:

The aim of this work was to synthesise pure and La-doped nickel oxide NiO thin films at different concentrations, and to study the effect of doping on the physical and optical properties of the samples produced for optoelectronic applications.

To achieve this, a thin film samples was prepared using spin coating technique of sol-gel derived solution onto glass substrates, namely pure NiO film and NiO samples doped with lanthanum La at concentrations of 3%, 6% and 9%. The choice of these concentrations was made in order to cover the areas of low, medium and high doping, all the samples was annealed at temperature 500°C.

The results obtained have enabled us to demonstrate the effect of crystallite size reduction and variation in optical band gap energy on the physical and optical properties of nickel oxide on the optoelectronic applications.

XRD analysis reveals that the films are polycrystalline with preferred growth along (111) plane. Microstructural analytical findings revealed that the average crystallite size (*D*) of samples decreases from 26.7 nm to 5.5 nm according to increased La concentration. Dislocation density and micro-strain increase with increasing La contents.

Films were transparent in the visible region and their transmittance decreased from 73% of pure NiO to 18% of 9% La-doped NiO, it is understood that the growth of La inhibits transmittance. The effect of doping on the width of the optical band gap led us to conclude that doping with lanthanum decreases the gap width as a function of dopant concentration, where the optical band gap was found to be in the range of 3.82 to 3.63 eV. The urbach energy values indicate that the obtained optical band gap is governed with the disorder variation in the NiO: La films.

Moreover, it was confirmed an enhancement of electrical conductivity with La doping, where sheet resistance of the films was measured at room temperature decreased to 0.696 $x10^6$ (Ω/square). All spin-coated samples having p-type conductivity. The results prove that the properties of LNO thin film are suitable for optoelectronic applications.

References

References

[1] N. Taiba, D. Tayyiba. The role of some important metal oxide nanoparticles for wastewater and antibacterial applications: A review. Environmental Chemistry and Ecotoxicology, Vol 3, (2021), 59-75.

[2] C.G. Granqvist, A. Hultaker, Transparent and conducting ITO films: new developments and applications. Thin Solid Films, Vol 411, (2002), 1-5.

[3] Z. Chen, T. Dedova, I.O. Acik, M. Danilson, M. Krunks, Nickel oxide films by chemical spray: Effect of deposition temperature and solvent type on structural, optical, and surface properties. Applied Surface Science, Vol 548, (2021), 149118.

[4] A. Nattestad, A.J. Mozer, M.K. Fischer, Y.B. Cheng, A. Mishra, P. Baeuerle, U. Bach. Highly efficient photocathodes for dye-sensitized tandem solar cells. Nat. Mat, Vol 9, (2010), 31-35.

[5] S. Jana, S. Samai, B.C. Mitra, P. Bera, A. Mondal, Nickel oxide thin film from electrodeposited nickel sulfide thin film: peroxide sensing and photo-decomposition of phenol. Dalton Transactions, Vol 43, (2014), 13096-13104.

[6] C.G. Granqvist, G.A. Niklasson, A. Azens, Electrochromics: Fundamentals and energy-related applications of oxide-based devices. Applied Physics A, Vol 89, (2007), 29-35.

[7] R. Zamiri, A.F. Lemos, A. Reblo, H.A. Ahangar, J.M.F. Ferreira, Effects of rare-earth (Er, La and Yb) doping on morphology and structure properties of ZnO nanostructures prepared by wet chemical method. Ceramics International. Vol 40, (2014), 523–529.

[8] J. L. Mason, H. Harb, J. E. Topolski, H. P. Hratchian and C. C. Jarrold. Photoelectron Spectra of Gd2O2– and Nonmonotonic Photon-Energy-Dependent Variations in Populations of Close-Lying Neutral States. The Journal of Physical Chemistry A, Vol 125, (2021), 857–866.

[9] E. Pikalova, A. Kolchugin, V. Tsvinkinberg, V. Sereda, A. Khrustov and E. Filonova. Comprehensive study of functional properties and electrochemical performance of layered lanthanum nickelate substituted with rare-earth elements. J. Power Sources, Vol 581, (2023), 233505.

[10] V. Ganesh, L. Haritha, M. A. Manthrammel, M. Shkir and S. AlFaify. An impact of La doping content on physical properties of NiO films facilely casted through spin-coater for optoelectronics. Physica B: Condensed Matter, Vol 582, (2020), 411955.

[11] J. Jia, F. Luo, C. Gao, C. Suo, X. Wang, H. Song, X. Hu, Synthesis of La-doped NiO nanofibers and their electrochemical properties as electrode for supercapacitors. Ceramics International, Vol 40, (2014), 6973-6977.

[12] R. G. Gordon. Criteria for Choosing Transparent Conductors. MRS Bull, Vol 25, (2000), 52–57.

[13] K. Chopra, L. Major, D. K. Pandya. Transparent conductors—a status review. Thin solid films, Vol 102, (1983), 1-46.

[14] Van Sark, W. G. J. H. M., Korte, L., & Roca, F. (Eds.). Physics and Technology of Amorphous-Crystalline Heterostructure Silicon Solar Cells. Engineering Materials, (2012), 301.

[15] Van Sark, W. G. J. H. M., Korte, L., & Roca, F. (Eds.). Physics and Technology of Amorphous-Crystalline Heterostructure Silicon Solar Cells. Engineering Materials, (2012), 302.

[16] A. Zunger, Practical doping principles. Applied Physics Letters, Vol 83, (2003), 57–59.

[17] A. Moustaghfir. Élaboration et caractérisation de couches minces d'oxyde de zinc application à la photoprotection du polycarbonate. Matériaux. Thése doctorat, Université Blaise Pascal- Clermont-Ferrand II, 2004. Français. NNT: tel-00012168.

[18] R. G. Gordon. Criteria for Choosing Transparent Conductors. MRS Bull, Vol 25, (2000), 52–57.

[19] Afzal Khan. Synthesis of Strontium Cuprate (SrCu2O) by MOCVD as a P-type Transparent Conducting Oxide Thin Film. Materials. Université de Grenoble, 2011. English. NNT: 2011GRENI008. tel-00582901.

[20] E. Savarimuthu, KC. Lalithambika, A. Moses Ezhil Raj, LC. Nehru, S. Ramamurthy, A. Thayumanavan, C. Sanjeeviraja, M. Jayachandran, Synthesis and materials properties of transparent conducting In_2O_3 films prepared by sol–gel-spin coating technique. Journal of Physics and Chemistry of Solids, Vol 68, (2007), 1380–1389.

[21] R. G. Gordon. Criteria for Choosing Transparent Conductors. MRS Bull, Vol 25, (2000), 52–57.

[22] K. Sreenivas, T. S. Rao, A. Mansingh, S. Chandra. Preparation and characterization of RF sputtered indium tin oxide films. J. Appl. Phys, Vol 57, (1985), 384.

[23] J. C. Manifacier. Thin metallic oxides as transparent conductors. Thin Solid Films, Vol 90, (1982), 297.

[24] K.L. Chopra, S. Major, D.K. Pandya. Transparent conductors: A status review, Thin Solid Films, Vol 102, (1983), 1-46.

[25] A. L. Dawar, J. C. Joshi. Semiconducting transparent thin films: their properties and applications, J. Mater. Sci., Vol 19, (1984), 1.

[26] S. Calnan, H. M. Upadhyaya, S. Buecheler, G. Khrypunov, A. Chiril, A. Romeo, R. Hashimoto, T. Nakada, and A. N. Tiwari. Application of high mobility transparent conductors to enhance long wavelength transparency of the intermediate solar cell in multi-junction solar cells. Thin Solid Films, Vol 517, (2009), 2340-2343.

[27] H. Habis, Z. Jean, A. Michel,. Transparent Conductive Oxides. Part I. General Review of Structural, Electrical and Optical Properties of TCOs Related to the Growth Techniques, Materials and Dopants. Defect and Diffusion Forum (Online), (2022), 417, pp.243-256. 10.4028/p97c472. hal-03759777

[28] A.B Kunz, Electronic structure of NiO. Journal of Physics C: Solid State Physics, Vol 14, (1981), L455–L460.

[29] MAM. Hussein, Effect of magnetization on ferrromagnetic and antiferromagnetic for NiO properties using quantum ESPRESSO package [Master's dissertation]. Khartoum: Sudan University of Science and Technology, (2016).

[30] H. Sato, T. Minami, S. Takata, & T. Yamada, Transparent conducting p-type NiO thin films prepared by magnetron sputtering. Thin Solid Films, Vol 236, (1993), 27–31.

[31] N. Rinaldi-Montes, P. Gorria, D. Martínez-Blanco, A.B. Fuertes, I. Puente-Orench, L. Olivi, & J.A. Blanco, Size effects on the Néel temperature of antiferromagnetic NiO nanoparticles. AIP Advances, Vol 6, (2016), 056104.

[32] B. Sasi. Preparation and characterization studies of nanostructured nickel oxide and lithium doped nickel oxide thin films. PhD thesis, University of Kerala, (2007).

[33] Z. Zhiwei. Oxygen reduction on lithiated nickel oxide as a catalyst and catalyst support. PhD thesis, Case Western Reserve University. (1993).

[34] A.J Hassan, Study of Optical and Electrical Properties of Nickel Oxide (NiO) Thin Films Deposited by Using a Spray Pyrolysis Technique. Jou. Mod Physics, Vol 05, (2014), 2184–2191.

[35] N. Tsuda, K. Nasu, A. Fujimori, K. Siratori, Introduction. In: Electronic Conduction in Oxides. Springer Series in Solid-State Sciences, Vol 94. (2000).

[36] R. J. Powell, W. E. Spicer. Optical Properties of NiO and CoO, Physical Review B (Solid State), Vol 2, (1970), 2182.

[37] H.A.E. Hagelin-Weaver, J.F. Weaver, G.B. Hoflund, G.N. Salaita. Electron energy loss spectroscopic investigation of Ni metal and NiO before and after surface reduction by Ar^{+} bombardment. Journal of Electron Spectroscopy and Related Phenomena. Vol 134, (2004), 139.

[38] K.S. Lee, H.J. Koo, K.H. Ham, W.S. Ahn. Crystal Molecular Orbital Calculation of the Lanthanum Nickel Oxide by Means of the Micro-Soft Fortran. Bull. Korean. Chem. Soc. Vol 16, (1995), 164.

[39] S. Hüfner, & Riesterer, T. Electronic structure of NiO. Physical Review B. Vol 33, (1986), 7267–7269.

[40] A.R. Williams, J. Kübler, & K. Terakura, Physical Review Letters, Vol 54, (1985), 2728–2728.

[41] R. Merlin, Electronic Structure of NiO. Physical Review Letters, Vol 54, (1985), 2727.

[42] W.L Roth, Magnetic Structures of MnO, FeO, CoO, and NiO. Physical Review. Vol 110, (1958), 1333–1341.

[43] M.T. Hutchings, & E.J. Samuelsen, Measurement of Spin-Wave Dispersion in NiO by Inelastic Neutron Scattering and Its Relation to Magnetic Properties. Physical Review B. Vol 6, (1972), 3447–3461.

[44] N. Mironova-Ulmane, V. Skvortsova, A. Kuzmin, Magnetic ion exchange interactions in NiO-MgO solid solutions. Phys. Solid State, Vol 47, (2005), 1516–1522.

[45] V. Massarotti, D. Capsoni, V. Berbenni, R. Riccardi, A. Marini, E. Antolini, Z. Structural and microstructural study of the formation of the solid solution LixNi1−xO. Naturforsch. Vol 46a, (1991), 503.

[46] S. Mørup, D. E. Madsen, C. Frandsen, C. R. H. Bahl, M. F. Hansen. Experimental and theoretical studies of nanoparticles of antiferromagnetic materials. Journal of Physics: Condensed Matter, Vol 19, (2007), 213202.

[47] Li L, Chen L, Qihe R, Li G (2006). Magnetic crossover of NiO nanocrystals at room temperature. Appl. Phys. Lett., Vol 89, (2006), 134102-3.

[48] RH. Kodama, SA. Makhlouf, AE. Berkowitz, Finite size effects in antiferromagnetic NiO nanoparticles. Phys. Rev. Lett., Vol 79, (1997), 1393-1396.

[49] SD. Tiwari, KP. Rajeev, Signatures of spin-glass freezing in NiO nanoparticles. Phys. Rev. B, Vol 72, (2005), 104433-9.

[50] SD. Tiwari, KP. Rajeev, Magnetic properties of NiO nanoparticles. Thin Solid Films, Vol 505, (2006), 113-117.

[51] K. Arai, T. Okuda, A. Tanaka, M. Kotsugi, K. Fukumoto, T. Ohkochi, T. Kinoshita, Three-dimensional spin orientation in antiferromagnetic domain walls of NiO studied by x-ray magnetic linear dichroism photoemission electron microscopy. Physical Review B, Vol 85, (2012), 104418.

[52] K. H. L. Zhang, K. Xi, M. G. Blamire, and R. G. Egdell. P -type transparent conducting oxides. J. Phys. Condens. Matter, Vol 28, (2016), p-38, 383002.

[53] Z. Xue, X. Liu, N. Zhang, H. Chen, X. Zheng, H. Wang, & X. Guo, High-Performance NiO/Ag/NiO Transparent Electrodes for Flexible Organic Photovoltaic Cells. ACS Applied Materials & Interfaces, Vol 6, (2014), 16403–16408.

[54] Z. He, C. Zhong, S. Su, M. Xu, H. Wu, Y. Cao, Enhanced Power-Conversion Efficiency in Polymer Solar Cells Using an Inverted Device Structure. Nat. Photonics, Vol 6, (2012), 591−595.

[55] W. Li, A. Furlan, k.H. Hendriks, M.M. Wienk, & R.A.J. Janssen, Efficient Tandem and Triple-Junction Polymer Solar Cells. Journal of the American Chemical Society, Vol 135, (2013), 5529–5532.

[56] K. Nomura, H. Ohta, A. Takagi, T. Kamiya, M. Hirano, H. Hosono. Room-temperature fabrication of transparent flexible thin-film transistors using amorphous oxide semiconductors. Nature, Vol 432, (2004), 488–492.

[57] H. Hosono. Recent progress in transparent oxide semiconductors: materials and device application, Thin Solid Films, Vol 515, (2007), 6000–6014.

[58] S. Lany, J. Osorio-Guillén, A. Zunger. Origins of the doping asymmetry in oxides: hole doping in NiO versus electron doping in ZnO. Phys. Rev. B, Vol 75, (2007), 241203.

[59] R. Lo Nigro, S. Battiato, G. Greco, P. Fiorenza, F. Roccaforte, G. Malandrino. Metal organic chemical vapor deposition of nickel oxide thin films for wide band gap device technology. Thin Solid Films, Vol 563, (2014), 50–55.

[60] Y. Chen, Y. Sun, X. Dai, B. Zhang, Z. Ye, M. Wang, & H. Wu, Tunable electrical properties of NiO thin films and p-type thin-film transistors. Thin Solid Films, Vol 592, (2015), 195–199.

[61] S. Chen, R. Liu, Y. Liu, S. Ho. Chen, J. H. Kim, and F. So. Nickel Oxide Hole Injection/Transport Layers for Efficient Solution- Processed Organic Light Emitting Diodes. Chem. Mater, Vol. 26, (2014), 4528–4534.

[62] S. Liu, R. Liu, Y. Chen, S. Ho, J.H. Kim, & F. So, Nickel Oxide Hole Injection/Transport Layers for Efficient Solution-Processed Organic Light-Emitting Diodes. Chemistry of Materials, Vol 26, (2014), 4528–4534.

[63] S. Årman. Electrochromic materials for display applications: An introduction. J. New Mater. Electrochem. Syst, Vol 4, (2001), 173–179.

[64] D. F. Goodchild, R. G., Webb, J. B., Williams. Electrical Properties of Highly Conducting and Transparent Thin Films of Magnetron Sputtered SnO2. J. Appl. Phys, Vol 57, (1985), 2308.

[65] K.J. Patel, G.G. Bhatt, J.R. Ray, P. Suryavanshi, & C.J. Panchal, All-inorganic solid-state electrochromic devices: a review. Journal of Solid State Electrochemistry, Vol 21, (2016), 337–347.

[66] H. Huang, J. Tian, W.K. Zhang, Y.P. Gan, X.Y Tao, X.H. Xia, & J.P. Tu, Electrochromic properties of porous NiO thin film as a counter electrode for NiO/WO3 complementary electrochromic window. Electrochimica Acta, Vol 56, (2011), 4281–4286.

[67] H. Moulki. Matériaux et dispositifs électrochromes à base de NiO modifié en couches minces. Thèse de doctorat, Université de Bordeaux, (2013), p-147.

[68] W. Tang et D. C. Cameron. Aluminum-doped zinc oxide transparent conductors deposited by the sol-gel process. Thin Solid Films, Vol. 238, (1994), 83-87.

[69] R. Wang, A. W. Sleight, et D. Cleary. High Conductivity in Gallium-Doped Zinc Oxide Powders. Chem. Mater., Vol 8, (1996), 433-439.

[70] W. Chia-Ching et Y. Cheng-Fu. Investigation of the properties of nanostructured Li doped NiO films using the modified spray pyrolysis method. Nanoscale Research Letters, Vol 8, (2013), 33.

[71] H. Moulki. Matériaux et dispositifs électrochromes à base de NiO modifié en couches minces. Thèse de doctorat, Université de Bordeaux, (2013), p-147.

[72] J. L. Mason, H. Harb, J. E. Topolski, H. P. Hratchian, and C. C. Jarrold. Exceptionally Complex Electronic Structures of Lanthanide Oxides and Small Molecules. Acc. Chem. Res. Vol 52, (2019), 3265-3273.

[73] E. Pikalova, A. Kolchugin, V. Tsvinkinberg, V. Sereda, A. Khrustov and E. Filonova. Comprehensive study of functional properties and electrochemical performance of layered lanthanum nickelate substituted with rare-earth elements. J Power Sources, Vol 581, (2023), 233505.

[74] R. Alan, L. Kok Loong, Structure-property Relations in Nonferrous Metals. Wiley Interscience, Vol 1, (2005), p-434.

[75] S. Aejitha, G. Dhanraj, T. Govindaraj, F. Maiz, M. Shkir, W. K. Kim, V. R. M. Reddy and D. H. Kim. Effect of La-doping on NiO photocatalyst for enhancing photocatalytic degradation performance under visible light irradiation: DFT calculations and degradation mechanism. Inorganic Chemistry Communications, Vol 156, (2023), 111172.

[76] V. Ganesh, L. Haritha, M. A. Manthrammel, M. Shkir and S. AlFaify. An impact of La doping content on physical properties of NiO films facilely casted through spin-coater for optoelectronics. Physica B: Condensed Matter, Vol 582, (2020), 411955.

[77] K. V. Chandekar, M. Shkir, A. Khan, M. Sayed, N. Alotaibi, T. Alshahrani, H. Algarni and S. AlFaify. Significant and systematic impact of yttrium doping on physical properties of nickel oxide nanoparticles for optoelectronics applications. Journal of Materials Research and Technology, Vol 15, (2021), 2584-2600.

[78] S. Senroy. Characterization of copper oxide, titanium oxide and copper doped titanium oxide thin films prepared by spray pyrolysis technique, PhD thesis, Bangladesh University, (2016).

[79] M. Nesa, Characterization of zinc doped copper oxide thin films synthesized by spray pyrolysis technique. Master memoir, Bangladesh University, (2016).

[80] K. Oura, M. Katayama, A.V. Zotov, V.G. Lifshits, A.A. Saranin, Growth of Thin Films. In: Surface Science. Springer, Advanced Texts in Physics, (2003), p 357-387.

[81] D.M. Mattox, Handbook of Physical Vapor Deposition Processing, Noyes Publications, NJ (1998).

[82] A. Marty et S. Andrieu. Croissance et structure des couches minces. Journal de Physique IV, Vol 06, (1996), pp.C7 3-11.

[83] G.C Righini, A. Chiappini, Glass optical waveguides: A review of fabrication techniques. Opt. Eng, Vol 53, (2014), 071819.

[84] A. Khan, Synthèse de Cuprates de Strontium ($SrCu_2O$) par MOCVD comme couche mince d'oxyde transparent conducteur de type P. PhD thesis, Grenoble University, (2006).

[85] C. Brinker and G. Scherer. Sol-Gel Science: The Physics and Chemistry of Sol-Gel Processing. Advanced Materials, Vol. 3, (1992), p-912.

[86] A. C. Pierre. Introduction to Sol-gel Processing. Springer Science, Vol 1, (1998).

[87] J.P. Chatelon, C. Terrier, J.A. Roger. Influence of elaboration parameters on the properties of tin oxide films obtained by the sol-gel process. Journal of Sol-Gel Science and Technology, Vol 10, (1997), 55e65.

[88] D. Frederichi, M.H.N.O. Scaliante, & R. Bergamasco, Structured photocatalytic systems: photocatalytic coatings on low-cost structures for treatment of water contaminated with micropollutants, a short review. Environmental Science and Pollution Research, Vol 28, (2020), 23610–23633.

[89] F B.W. Shivaraj, H.N. Narasimha Murthy, M. Krishna, S.C. Sharma. Investigation of influence of spin coating parameters ont eh morphology of ZnO thin films by Taguchi method. International Journal of Thin Films Science and Technology, Vol 2, (2013), 143e154.

[90] J. Shojaeiarani, D. Bajwa, N.M. Stark, T.M. Bergholz, & A.L. Kraft, Spin coating method improved the performance characteristics of films obtained from poly (lactic acid) and cellulose nanocrystals. Sustainable Materials and Technologies, Vol 26, (2020), e00212.

[91] L. Cattin, B.A Reguig, A. Khelil. Properties of NiO thin films deposited by chemical spray pyrolysis using different precursor solutions. Appl Surf Sci, Vol 254, (2008), 5814-5821.

[92] H. Kamal, E.K. Elmaghraly, S.A. Ali. The electrochromic behavior of nickel oxide films sprayed at different preparative conditions. Thin Solid Films, Vol 483, (2005), 330-339.

[93] A. Boukhachem, R. Boughalmi, M. Karyaoui. Study of substrate temperature effects on structural, optical, mechanical and opto-thermal properties of NiO sprayed semiconductor thin films. Materials science and engineering: B, Vol 188, (2014), 72-77.

[94] S. Kasuma, W. Ningsih. Effect of various solvent on the synthesis of NiO nanopowders by simple sol-gel methods and its characterization. Indones. J. Chem, Vol 15, (2015), 50-55.

[95] D. Nikolić, M. Panjan, G.R. Blake. Annealing-dependent structural and magnetic properties of nickel oxide (NiO) nanoparticles in a silica matrix. journal of the European ceramic society, Vol 35, (2015), 3843-3852.

[96] P. Ravikumar, B. Kisan, A. Perumal. Thickness dependent ferromagnetism in thermally decomposed NiO thin films. journal of magnetism and magnetic materials, vol 418, (2016), 86-91.

[97] M.A. Aegerter, & M. Mennig (Eds.), Sol-Gel Technologies for Glass Producers and Users, (2004).

[98] Spin Coating: infinity PV, Denmark., http://plasticphotovoltaics.org/lc/lc-fabrication/lc-coating/lc-spin.html. (accessed 10.10.18).

[99] N. Sahu, B. Parija, S. Panigrahi. Fundamental understanding and modeling of spin coating process: a review. Ind. J. Phys, Vol 83, (2009), 493502.

[100] L.A. Dobrzanski, M. Szindler. Sol gel TiO_2 antireflection coatings for silicon solar cells. J. Achieve. Mater. Manuf. Eng, Vol 52, (2012), 714.

[101] E. Mikuli, A. Migdał-Mikuli, R. Chyży, B. Grad, & R. Dziembaj, Melting and thermal decomposition of [Ni $(H_2O)_6$] $(NO_3)_2$. Thermochimica Acta, Vol 370, (2001), 65–71.

[102] A. M. Soleimanpour and A. H. Jayatissa. Preparation of nanocrystalline nickel oxide thin films by sol-gel process for hydrogen sensor applications. Mater. Sci. Eng. C, Vol 32, (2012), 2230–2234.

[103] S. Mohd, Z.R. Khan, M.S. Hamdy, H. Algarni, S. AlFaify, A facile microwave assisted synthesis of $PbMoO_4$ nanoparticles and their key characteristics analysis: a good contender for photocatalytic applications. Mater. Res. Express, Vol 5, (2018), 095032.

[104] S. AlFaify, M. Shkir. A facile one pot synthesis of novel pure and Cd doped PbI_2 nanostructures for electro-optic and radiation detection applications. Opt. Mater, Vol 88, (2019), 417–423.

[105] M. Shakir, S. Kushwaha, K. Maurya, G. Bhagavannarayana, M. Wahab. Characterization of ZnSe nanoparticles synthesized by microwave heating process. Solid State Commun, Vol 149, (2009), 2047–2049.

[106] M. Shkir, M.S. Hamdy, S. AlFaify, A facile one pot flash combustion synthesis of ZnO nanoparticles and their characterizations for photocatalytic applications, J. Mol. Struct, Vol 1197, (2019), 610–616.

[107] M. Shkir, M.T. Khan, A. Khan, A.M. El-Toni, A. Aldalbahi, S. AlFaify. Facilely synthesized Cu: PbS nanoparticles and their structural, morphological, optical, dielectric and electrical studies for optoelectronic applications. Mater. Sci. Semicond. Process, Vol 96, (2019), 16–23.

[108] M. Shkir, S. Aarya, R. Singh, M. Arora, G. Bhagavan narayana, T. Senguttuvan. Synthesis of ZnTe nanoparticles by microwave irradiation technique, and their characterization. Nanosci. Nanotechnol. Lett, Vol 4, (2012), 405–408.

[109] V. Ganesh, L. Haritha, M. Anis, M. Shkir, I.S. Yahia, A. Singh, S. AlFaify. Structural, morphological, optical and third order nonlinear optical response of spin-coated NiO thin films: an effect of N doping. Solid State Sci, Vol 86, (2018), 98–106.

[110] B.E. Sernelius, K.F. Berggren, Z.C. Jin, I. Hamberg, C.G. Granqvist. Band-gap tailoring of ZnO by means of heavy Al doping. Phys. Rev. B, Vol 37, (1988), 10244–10248.

[111] R. Dalven. Empirical relation between energy gap and lattice constant in cubic semiconductors. Phys. Rev. B, Vol 8, (1973), 6033–6034.

[112] S. Chandramohan, A. Kanjilal, J. K. Tripathi, S. N.Sarangi, R. Sathyamoorthy, and T. Som. Structural and optical properties of Mn-doped CdS thin films prepared by ion implantation. Journal of Applied Physics, Vol 105, (2009), 1-4.

[113] D. Adler and J. Feinleib. Electrical and optical properties of narrow-band materials. Phys. Rev. B, Vol 2, (1970), p 3112–3134.

[114] S.A. Makhlouf, M.A. Kassem, M.A. Abdel-Rahim. Crystallite size dependent optical properties of nanostructured NiO films. Optoelectronics and Advanced Materials, Vol 4, (2010), 1562.

[115] S. Benramache, A. Rahal and B. Benhaoua. The effects of solvent nature on spray deposited ZnO thin film prepared from Zn $(CH_3COO)_2$, $2H_2O$. Optik, Vol 125, (2014), 663-666.

[116] S. Nandy, B. Saha, M. K. Mitra and K. K. Chattopadhyay. Effect of oxygen partial pressure on the electrical and optical properties of highly (200) oriented p-type $Ni_{1-x}O$ films by DC sputtering. Journal of Materials Science, Vol 42, (2007), 5766-5772.

REPUBLIQUE ALGERIENNE DEMOCRATIQUE ET POPULAIRE
MINISTERE DE L'ENSEIGNEMENT SUPERIEUR
ET DE LA RECHERCHE SCIENTIFIQUE
UNIVERSITE MOHAMED KHIDER - BISKRA
Faculté des SE&SNV
Département des Sciences de la matière
Filière: Physique

الجمهورية الجزائرية الديمقراطية الشعبية
وزارة التعليم العالي والبحث العلمي
جامعة محمد خيضر بسكرة
كلية العلوم الدقيقة وعلوم الطبيعة والحياة
قسم :علوم المادة
شعبة :الفيزياء

تصريـــح شرفـــي

خاص بالالتزام بقواعد النزاهة العلمية لإنجاز بحث

(ملحق القرار 1082 المؤرخ في 2021/12/27)

أنا الممضي أسفله،

السيد(ة): رقيحي عبد الحميد

الصفة: طالب سنة ثانية ماستر فيزياء تخصص: فيزياء المواد

الحامل(ة) لبطاقة التعريف الوطنية رقم: 203831052 الصادرة بتاريخ: 2018/12/12

المسجل بكلية: علوم المادة قسم: علوم المادة

والمكلف بانجاز أعمال بحث : مذكرة ماستر في الفيزياء

عنوانها: Study on the Structural, Optical and Electrical Properties of pure NiO and La-doped NiO prepared by sol-gel method.

أصرح بشرفي أني ألتزم بمراعاة المعايير العلمية والمنهجية ومعايير الأخلاقيات المهنية والنزاهة الأكاديمية المطلوبة في انجاز البحث المذكور أعلاه وفق ما ينص عليه القرار رقم 1082 المؤرخ في 2021/12/27 المحدد للقواعد المتعلقة بالوقاية من السرقة العلمية ومكافحتها.

التاريخ: 2024/02/22

إمضاء المعني بالأمر

Study on the Structural, Optical and Electrical Properties of pure NiO and La-doped NiO, prepared by sol-gel method.

Abstract:

We report an experimental study focuses on the synthesis and characterization of thin films of nickel oxide undoped and doped with lanthanum (La) prepared by sol-gel spin-coating technique on glass substrates annealed at temperature 500°C. The main objective is to provide a comprehensive study on the effect of the doping on the physical properties of this material. For that, we used Lanthanum (III) nitrate La $(NO_3)_3$ a as precursors, has a rate of doping was (3%, 6%, 9%). The structural, optical and electrical properties of the obtained films were characterized by various techniques.

X-ray diffraction analysis of pure an La-doped NiO thin films exhibit that the final films belonging to cubic structure, crystallize preferentially along (111) plane. The crystallite size represents the variations from 26.7 nm to 5.5 nm. The optical analysis shows that NiO: La films present a direct band gap energy value lying in the range of 3.63-3.82 eV. Also, the effect of the La incorporation in NiO matrix on the disorder is studied in terms of urbach energy. Finally, it has been found that La doping allows the improvement of the electrical conductivity, where the measurements of the sheet resistance of samples confirm that this Rs is the order of 10^9 (Ω/square) for pure NiO films, and are about 10^6 (Ω/square) for doped films.

Keywords: La doped NiO, metal oxide semiconductors (MOS), p-type transparent oxide thin films, sol–gel process, spin coating technique, XRD, physical properties, optoelectronic.

دراسة الخصائص البنيوية، الضوئية والكهربائية لأكسيد النيكل (NiO) النقي والمطعم بواسطة اللانثانوم (La-NiO) المحضر بتقنية صل-جل

ملخص:

نقدم تقريرًا عن دراسة تجريبية تركز على تركيب وتوصيف الأغشية الرقيقة لأكسيد النيكل غير النقي والمطعم باللانثانوم (La) المحضرة بتقنية صل- جل والطلاء الدوراني على مساند زجاجية ملدنة عند حرارة 500 درجة مئوية. الهدف الرئيسي هو تقديم دراسة شاملة عن تأثير التطعيم على الخواص الفيزيائية لهذه المادة. من أجل ذلك، استخدمنا نترات اللانثانوم ($Lanthanum\ (III)\ nitrate\ La\ (NO_3)_3$) كسلائف، وكان معدل التطعيم (3%، 6%، 9%). الخواص الهيكلية، البصرية والكهربائية للأفلام تم الحصول عليها بتقنيات مختلفة.

يُظهر تحليل انعراج الأشعة السينية للأغشية الرقيقة النقية لأكسيد النيكل النقي والمطعم بالانثانوم أن هذه الأغشية النهائية تنتمي إلى بنية مكعبة، تتبلور بشكل تفضيلي على طول المستوى (111). ويظهر حجم البلورات الاختلافات من 26.7 نانومتر إلى 5.5 نانومتر. يُظهر التحليل البصري أن أفلام (NiO: La) تقدم فاصل طاقي مباشرة ذو قيمة تقع في نطاق 3.82-63.3 فولت. كما تمت دراسة تأثير دمج (La) في مصفوفة NiO على الاضطراب من حيث طاقة أورباخ. أخيرًا، وجد أن التطعيم بواسطة La يسمح بتحسين التوصيل الكهربائي، حيث تؤكد قياسات مقاومة الصفائح للعينات Rs أنها هي في حدود 10^9 (Ω/square) لأفلام NiO النقية، وهي حوالي 10^6 (Ω/square) للأفلام المطعمة.

الكلمات المفتاحية: أكسيد النيكل المطعّم بالانثانوم (**La-NiO**)، أكاسيد المعدنية لأشباه موصلات (**MOS**)، الأغشية رقيقة للأكاسيد الشفافة من النوع **p**، عملية الصل- جل، تقنية الطلاء بالدوران، انعراج الأشعة السينية **XRD**، الخواص الفيزيائية، الإلكترونيات البصرية.